4-1998

A Comparison between Two Phase System and Single Phase System in Stiff Beveled Blade Coating by Measuring the Blade Forces

Ravi Mohan

A COMPARISON BETWEEN TWO PHASE SYSTEM AND SINGLE PHASE SYSTEM IN STIFF BEVELLED BLADE COATING BY MEASURING THE BLADE FORCES

by

Ravi Mohan

A Thesis
Submitted to the
Faculty of The Graduate College
in partial fulfillment of the
requirements for the
Degree of Master of Science
Department of Paper and Printing Science and Engineering

Western Michigan University
Kalamazoo, Michigan
April 1998

ACKNOWLEDGEMENTS

I wish to express a sincere appreciation and gratitude to my advisor, Dr. Brian Scheller, for his invaluable assistance, direction, motivation and support throughout this course work. I also thank and appreciate Dr. D. Qi and Dr. G. Wouch for their invaluable guidance and encouragement. I also thank Dr. R. Aravamuthan, Dr. D. K. Peterson and Dr. R. Janes, for their advice.

I also appreciate the help of Mr. R. Reams, Mr. M. Stoops, Mr. J. Kendrick, Mr. J. Singleton, Mr. G. Slator, Mr. A. Bihari, Mr. S. Bhatnagar and Mr. Hariharan for their precious help in the experiment.

Finally, my deepest gratitude and appreciation are extended to my parents and sisters for their love, sacrifice and support to bring this study to completion.

Ravi Mohan

A COMPARISON BETWEEN TWO PHASE SYSTEM AND SINGLE PHASE SYSTEM IN STIFF BEVELLED BLADE COATING BY MEASURING THE BLADE FORCES

Ravi Mohan, M. S.

Western Michigan University, 1998

The effect of pigment particle interactions in a two-phase system on blade force is investigated. Three coating colors of 0%, 40% , and 55% solids, of the same high shear viscosity and density, were tested for blade force, blade run-in relationship. The Cylindrical Laboratory Coater was used to blade coat the coating on a polyester film. Blade deflection was measured by placing a probe in direct contact with the back side of the blade. A calibration plot between blade force and blade deflection was then used to determine the actual blade forces. A statistical analysis of the data reveals that there is no significant difference between the single phase and two phase system. The viscosity, calculated at an estimated shear rate under the blade, has significant impact on the blade forces. At lower blade run-ins of 5 (5/1000 inch) and 10, the viscosity and blade force of the 0% solids were the greatest, followed by the 40%, and 55% solids. At the blade run-in of 15, the difference in the viscosity of all coating colors was reduced, as was the difference in the blade forces. The blade force of 0% solids was still higher than others. At blade run-in 20, there was no statistically significant evidence of differences in the blade forces and viscosity of all three coating colors.

TABLE OF CONTENTS

Table of Contents - Continued

CHAPTER

Table of Contents - Continued

CHAPTER

Table of Contents - Continued

CHAPTER

Table of Contents - Continued

LIST OF TABLES

LIST OF FIGURES

List of Figures - Continued

List of Figures - Continued

CHAPTER I

INTRODUCTION

Blade coating is a very popular technique for coating paper and paperboard for improving appearance and printability. The advantage of blade coating is that quality coating can be done at high speeds and different coat weights. For maximizing capital investment, it is always desirable to use the highest possible solids of coating color at the maximum speed without causing runnability problems.

Generally, coat weight applied on the paper will decrease by increasing the blade load and blade angle. It will also decrease by decreasing coater speed, blade thickness, coating colors viscosity or solids, and surface absorptivity or roughness of base paper. In the actual process, coat weight is controlled by adjusting the blade pressure or by reducing the solids content of the coating color. Many coating colors give satisfactory results at a particular speed, but at higher speed, weeps, spits, whiskers or stalagmites, coating scratches, streaks or difficulty in coat-weight uniformity in the cross machine direction can be experienced(1).

So as a general practice coating color solids are reduced, which not only increases the drying cost of coated paper, but potentially may increase binder migration into the paper web. At high solids, pigments and latex are retained in the coating layer and latex penetration into the web is prevented. The exact mechanisms involved in the

blade coating process and the limits on the coater speed are not well understood. Most of the mills rely on trial and error and on their own experience.

Several models had been proposed for analyzing the process of blade coating. There is no widely accepted model which can predict the resulting coat weight and maximum possible speed when the process conditions and the coating color rheological properties are known. However, it is widely accepted that the final coat weight on coated paper is the result of the balance between the color related forces and the deflection of the blade. There have been many attempts to measure or predict the blade forces. The dynamic blade forces can be calculated by measuring the blade deflection.

In this study, a comparison is done between two phase and single phase systems by measuring the blade deflection. For this a typical coating color and polymer solution of similar high shear viscosity has been applied on a polyester film by a Cylindrical Laboratory Coater (CLC).

CHAPTER II

LITERATURE REVIEW

1.Factors Affecting the Blade Coating

1.1Base Sheet Properties

A good quality base paper will always be the best means for improving the quality of the finished coated product. In practice, coated paper comprises a thin coating layer applied to a relatively thick fibrous web which has a rough surface and a porous structure. However, if the base stock has many defects it may affect properties of the final product. Apart from this, machine runnability also gets affected by poor base stock, because of its poor tensile, pickup strength, etc. The following are the some of very important base paper qualities which affect the coating operation.

1.1.1 Sheet Roughness

Although the effect of sheet roughness on the limit speeding of coating is not very well understood, it is very important parameter for blade coating. It represents the weight of coating which will be removed from the fluid mass in the coating process and will instantaneously deposit on the paper surface(2). The paper roughness is due to presence of hills and valleys present on paper surface. In the context of coating it can be

considered that those pores or pockets which are bigger then pigment particles will represent effective surface roughness volume(3) (Figure 1).

In normal blade coating, the blade may be touching the topmost fibers of the paper. In this case, the mass of coating which has access to the space between the blade and the base paper is no more than that available in the pores on the surface. This suggests that to a great extent the coat weight is controlled by the surface roughness volume. However, this may change with an increase on applied blade force. As the paper compresses due to blade force, the surface roughness volume will decrease. Hence the applied coat weight will also decrease with a decrease in the paper roughness. The coat weight can only be reduced to some minimum value by external blade pressure. There will always be some surface roughness on the paper surface, hence some minimum coat weight will occur even at very high blade force.

If the base paper can be made fully smooth so that it has negligible surface roughness volume, at very high blade loading there will be a situation that no coating will deposit on the paper surface and coat weight will go towards zero. Kahila and Eklund had carried out experiment on plastic-pigment coated paper which was made very smooth by supercalendering(2). It was observed that at a very high load, a very low coat weight was achieved (1gram/meter^2). But a coat weight of 10 gram/meter^2 was very difficult to achieve. They conducted the experiments on paper of different roughness and observed that as paper roughness increased, coat weight also increased(2) (Figure 2).

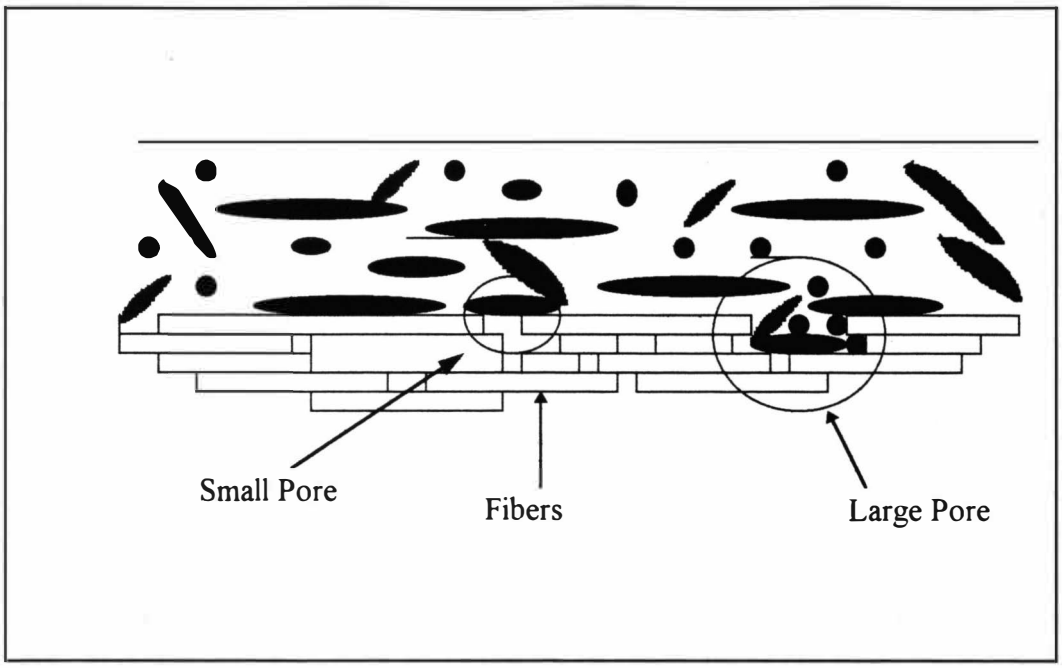

Figure 1. Effect of Base Sheet Roughness on Coating (7).

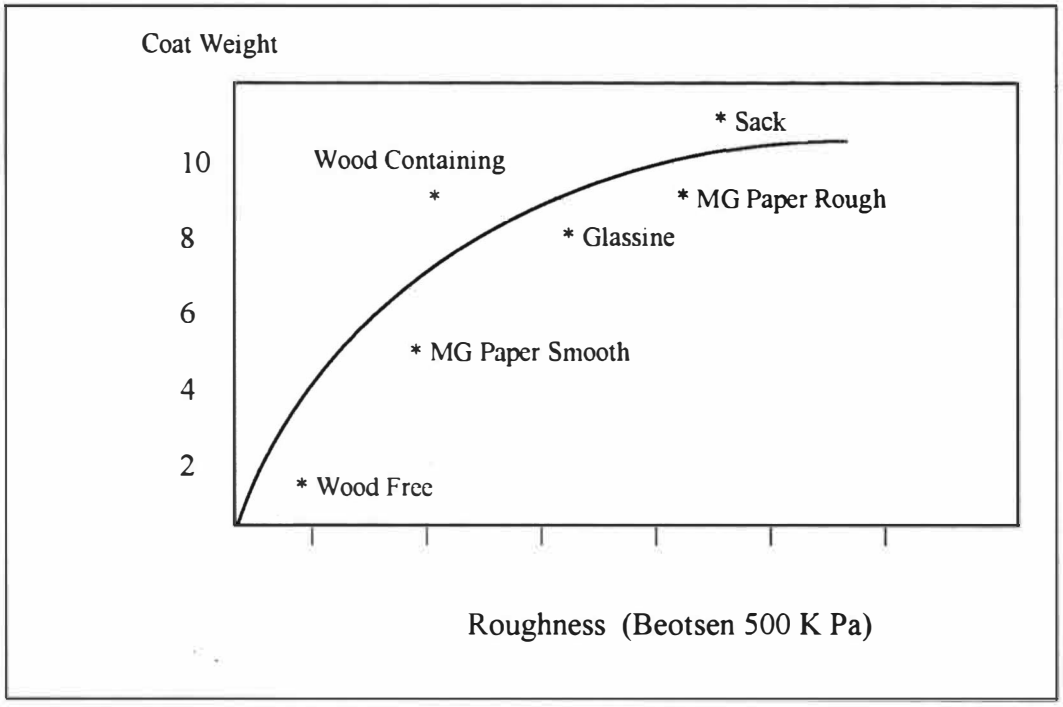

Figure 2. Dependence of Coat Weight Upon Paper Roughness (12).

In base paper, there are the pores which are very small in size in comparison to the pigment particle and hence do not contribute much in roughness volume of the paper. But these small pores will take away water from the coating formulation and a filtercake may form. The formation of a filter cake may be another limiting factor in high speed coating(3).

1.1.2 Sheet Absorbency

The higher the absorbency of paper, the greater will be the total coating pickup during coating. The absorbency of the sheet can be altered by sizing. Follete and Fowells(4) have done work on comparing two papers of different levels of sizing. They observed that papers with low sizing level picked up a higher coat weight. They also observed that when blade pressure was plotted against the coat weight, the slope decreased as sheet absorbency increased(14). This appears to be due to an increase in sheet absorbency causing more coating deposits on the surface (Figure 3). The sheet absorbency may also affect the surface roughness volume. As the swelling of fibers takes place, the roughness volume may increase and more coating is deposited on the paper surface.

1.1.3 Sheet Compressibility

The potential effect of base paper compression on the surface roughness volume of the paper has been mentioned in literature. As the paper compresses due to an external load, the roughness volume will decrease (Figure 4).

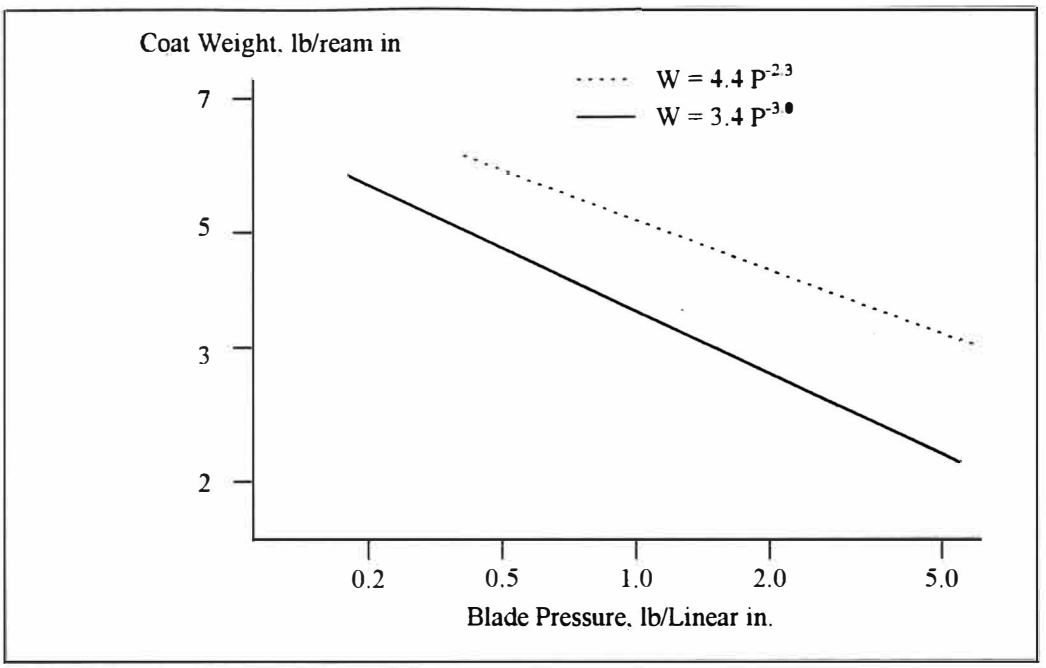

Figure 3. The Effect of Base Sheet Absorbency on the Blade Pressure and Coat Weight (14).

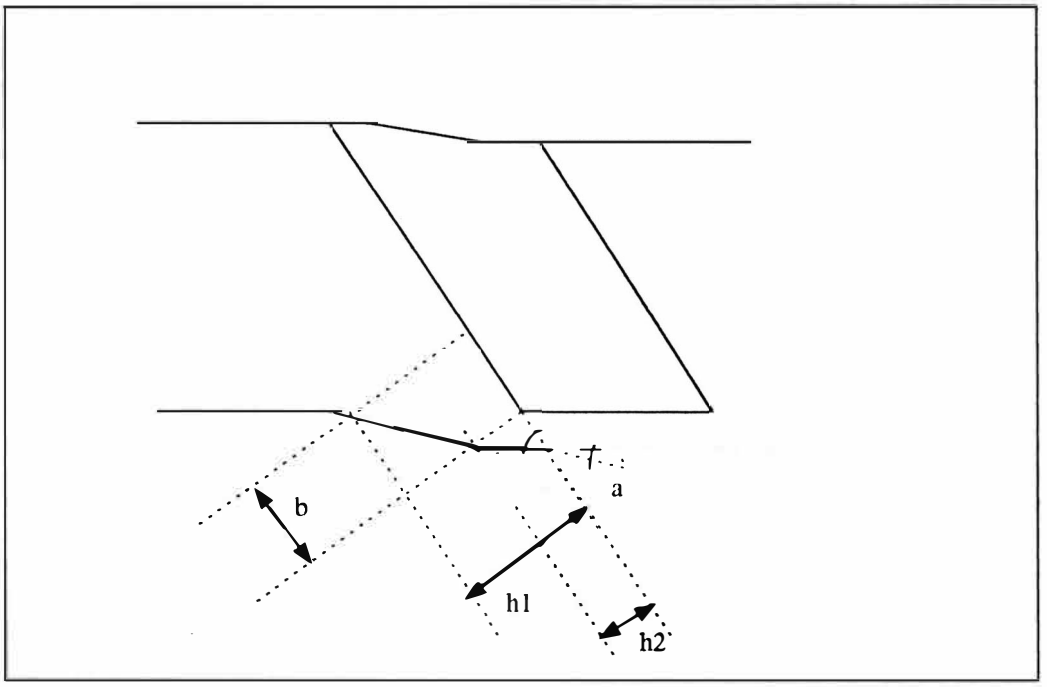

Figure 4. Possible Effect of Compression of the Paper (19).

Iskasson had experimentally found that compression can change the blade nip entrance region and has a large effect on the forces experienced by the blade(5). He found a correlation between the calculated blade forces and the experimentally determined wet film thickness. By using the theory of linear elasticity, blade force is calculated and it is found that the force the blade experiences during the coating should result in much higher deflection than that which corresponded to wet film thickness (5). It is possible that the blade compresses the base paper and rubber-covered backing roll, as shown in Figure 3. As a result of the compression of the base paper and the decrease in surface roughness, high color related forces can develop at the tip of the blade due to a converging entrance region. This compression of the paper will cause deformation of the paper surface near to the blade tip and will result in a very small angle between the paper and blade(6), resulting in a greater hydrodynamic force. This hydrodynamic force will try to lift the blade and in order to maintain the coat weight, a higher blade force is required. (Figure 4)

1.1.4 Sheet Porosity

As the layer of coating is deposited on the surface, most of the air on the paper surface is displaced. This displaced air will pass through the paper. As machine speed increases, the surface air will be required to be removed at a higher rate. If the paper is impermeable, then the speed of coating will be limited by the displacement of the air (7). But the pore space is also penetrated by liquid because of hydrodynamic force and by capillary pressure. This penetration of the liquid may cause entrainment of air and this air may be confined and compressed. The confinement and compression are most severe when

the substrate is pressed very hard against a backing roll. At the opposite extreme is the nonporous sheet. The porosity of the sheet will also affect the filtercake formation during the coating. If porosity of the sheet is very high, it may cause penetration of the latex and water into the substrate, leaving a deposited mass on the surface which will adversely affect the coating process(7).

1.2 Coating Blade

In the case of stiff beveled blade coater, coat weight applied to the base paper is influenced by the action of the blade. The excess coating applied to the paper is scrapped off by the blade.

As mentioned previously, coat weight is controlled by a balance between dynamic forces and the external force applied by the tube pressure. So the control of coat weight depends on the balance between blade loading and coating forces. The blade coating forces can be related to the deflection of the blade during coating(4). The blade itself can be regarded as cantilever beam with one end held by the blade holder and the other end subjected to a concentrated load P which depends upon the blade pressure(8). An expression of the deflection of beams has been given by Timoshenko(8) and applied to blade coating by Folllette and Fowells (4). In this case deflection is,

$$Y_{max} = \frac{KL^3}{3EI}$$

where K is the total load, E is the modulus of elasticity, L is the blade extension from the edge of the bottom lip of blade holder to the doctoring edge of the blade, and I is moment of inertia.

The moment of inertia I is given by,

$$I = \frac{c^3 b}{12}$$

where b is the blade width and c is the blade thickness.

From the above equation, the deflection of the blade will increase by increasing the blade extension(L), decreasing the width of the blade(b), decreasing the blade thickness(c), and using the material of lower modulus of elasticity (E) (Figure 5).

Other factors of the blade which can affect the blade coating are given below.

1.2.1 Bevel Surface Area

Kuzmak has worked with trailing blade coater with two different bevel surfaces, having the same thickness and blade stiffness. He found that on increasing the bevel length, coat weight increased (Figure 6) (9). He concluded that since the hydrodynamic force is directly proportional to the length of the bevelled surface, as beveled surface increases, the hydrodynamic force also increases. This hydrodynamic force works against the tube pressure and tries to lift the blade, hence higher coat weight is achieved.

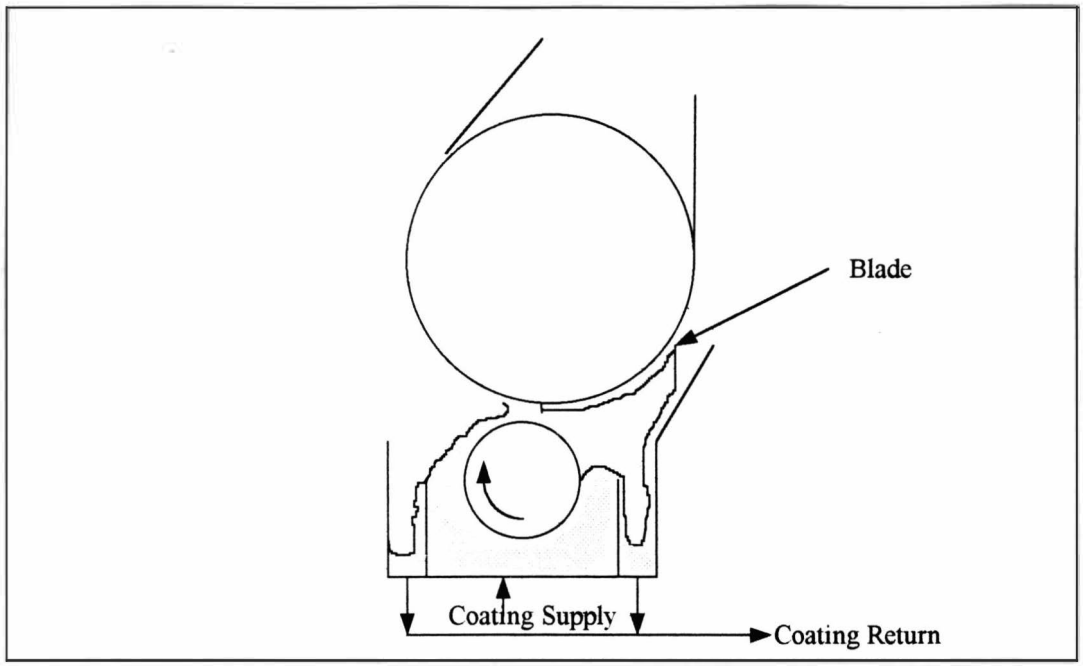

Figure 5. Flooded Nip Inverted Blade Coating (12).

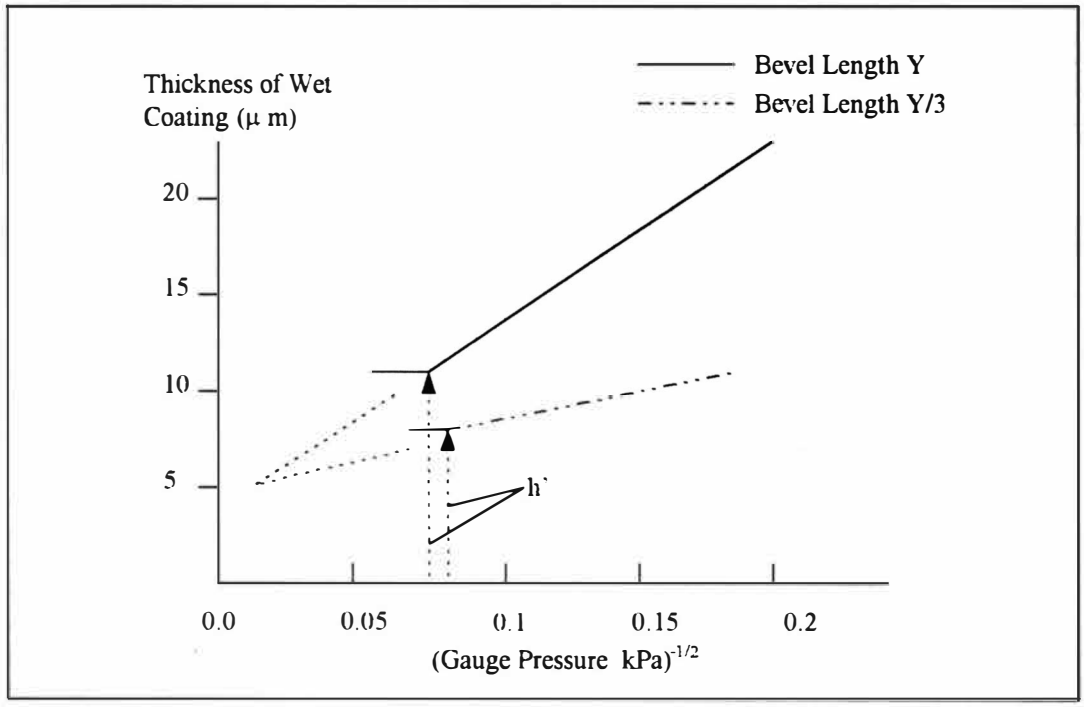

Figure 6. Effect of the Bevel Length on Wet Coating Thickness (22).

1.2.2 Blade Angle

Under normal circumstances, coating is done by keeping blade angle between 30 to 45 degrees. During coating, blade pressure transfers to the paper as shown in Figure 7. The force acting perpendicular to the base can be obtained by,

$$F_0 = F_z \mathrm{Cos}\alpha$$

where α is the blade angle.

So as the blade angle decreases, the perpendicular load on the paper increases and less coat weight will be deposited on the surface of paper.

1.2.3. Blade Nip Geometry

The blade can be in the contact of paper and backing roll in three positions as shown in the Figure 8: (a)Heel, (b)Land or (c)Toe. Running on the land is the optimum condition. Running on the heel will cause decrease in the coat weight(1). When blade runs on toe the bevel angle decreases because of the converging entrance, and less coat weight is deposited on the paper.

1.3 Coating Color Properties

Coating color is used to treat the surface of paper in order to provide smoothness and improved printing quality. High speed coaters require colors which have good rheology behavior at high shear, low dewatering and provide a defect free paper surface.

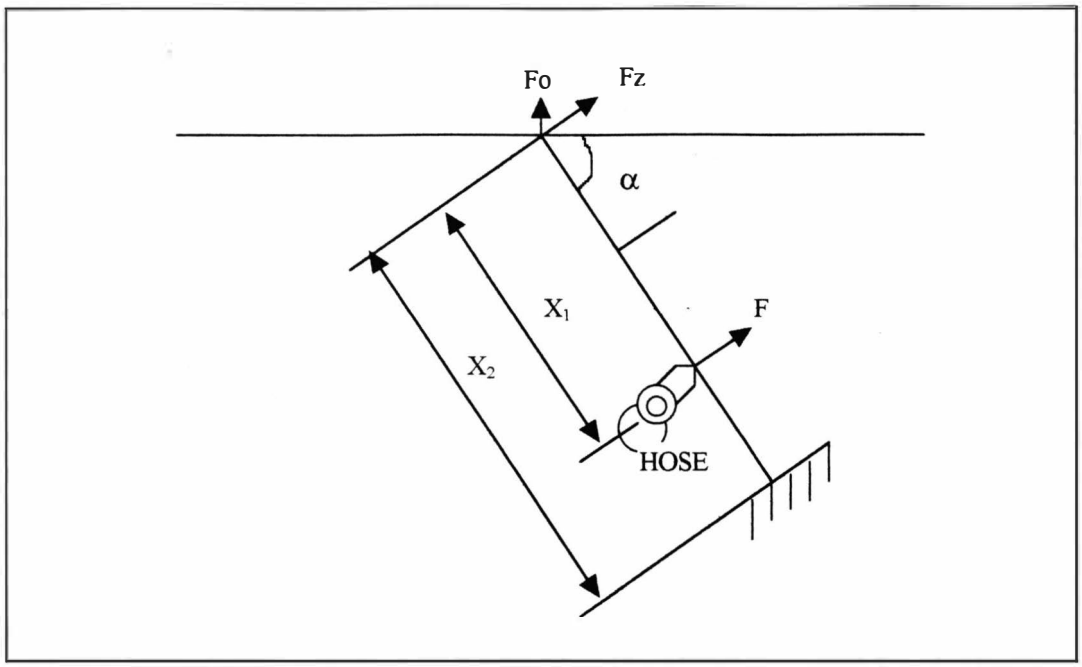

Figure 7. Blade Pressure Transmission to Paper (12).

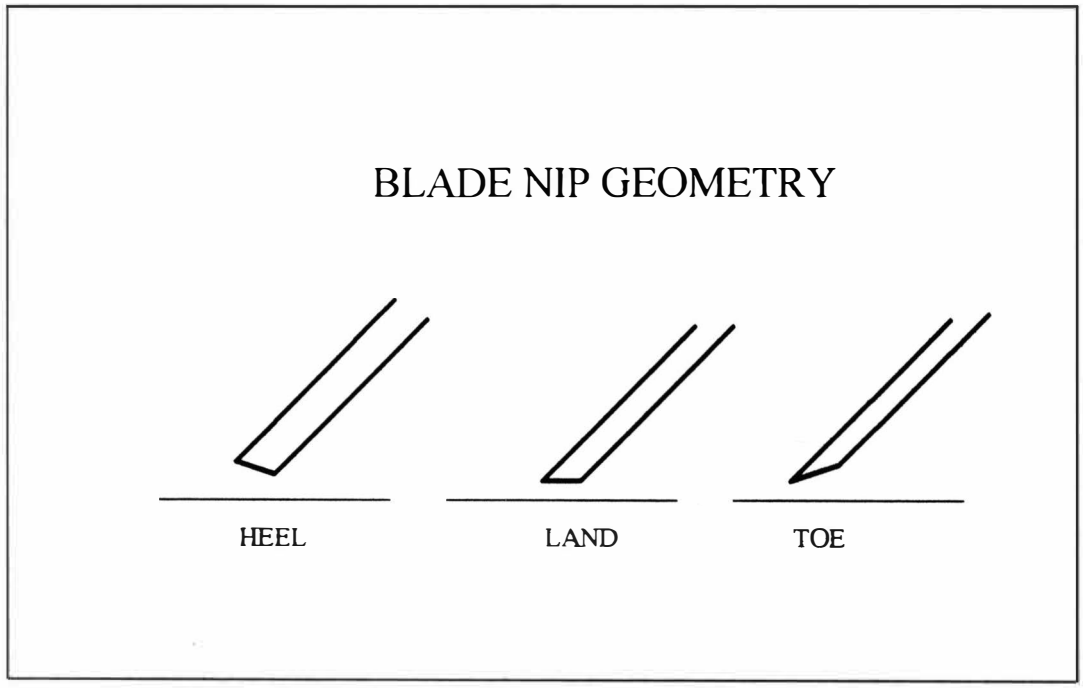

Figure 8. Definitions of Blade Nip Geometry (1).

The best fiber coverage with the lowest coating weight is desired and a bulky coating with good optical and mechanical properties will meet these requirements. There are the numerous factors which control the runnability of the coating process and the fiber coverage. The color formulation is certainly the most critical one. The coating color is a complex mixture of an inorganic pigment and polymeric synthetic binders in an aqueous slurry(10). The following properties are found to be very important in coating.

1.3.1 Water Retention

Water removal from the coating color during the coating process is a critical concern in coated paper production and has been the subject of many studies. It is of specific importance in blade coating operations, where excessive water loss to the base stock may cause runnability or quality defects such as scratching, bleeding, streaking (caused by undesired rheology and solids buildup), web breaks from weakening of the base stock, surface roughening due to fiber swelling, and print mottle(11). Consequently, prevention of excessive water loss is of keen interest to blade coating practitioners. The coating under pressure tends to move as a plug flow into the porous base stock. It will penetrate the larger pores, such as "pin holes," and then the small pores of paper. As a result, water and some binders will migrate into the paper medium, while the bulk of the pigments and other solids will be retained on the surface(12). Eventually a high solids filter cake will be formed near the interface, which may progressively grow in thickness as the coating continues to loose water. Meanwhile, capillary migration takes place after the

paper is wet by the coating water, until the coating is consolidated by the dryer. The extent of water loss in such a process may vary widely with coating formulation, base stock and sometimes machine settings. (Figure 9)

Eklund and Letzelter have proposed a model for the dewatering of coating colors based on modified Hagen-Poisseuille equation by taking color and machine parameters into account(13). They suggested that when coating is applied to the base sheet, there is penetration of the liquid phase of the coating color into the paper. The liquid phase consists of the dispersing medium (water) and of the soluble binders such as CMC, starch, etc. At the interface of the paper, an immobilized layer consisting of the coating pigment and all non-soluble components is formed. The solids content in this immobilized layer is higher than in the bulk of the color (Figure 10). The immobilized layers grow with dewatering, building up a structure that is denser than the bulk phase(13). The dewatering forces are capillary pressure, diffusion and external pressure. The dewatering depends on the base paper and machine configuration. If paper porosity is high then it will increase the dewatering.

However, the type of the pigment particles present in coating color, their size, and the packing structure in the immobilized color will also affect the dewatering. Water loss can be controlled very effectively through coating formulation design. Generally in the industry different thickening agents are used to increase the viscosity of coating colors. It also helps in reduction in water loss due to dewatering. Coating colors which uses protein as binding agent are also known for less water loss.

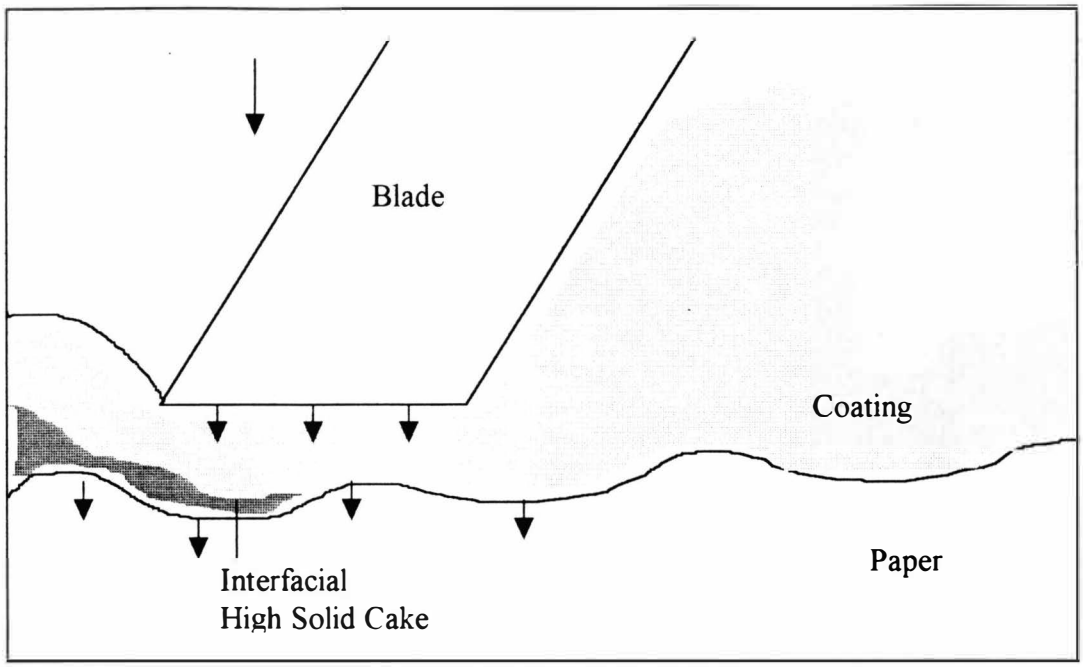

Figure 9. Coating Dewatering Under Blade (29).

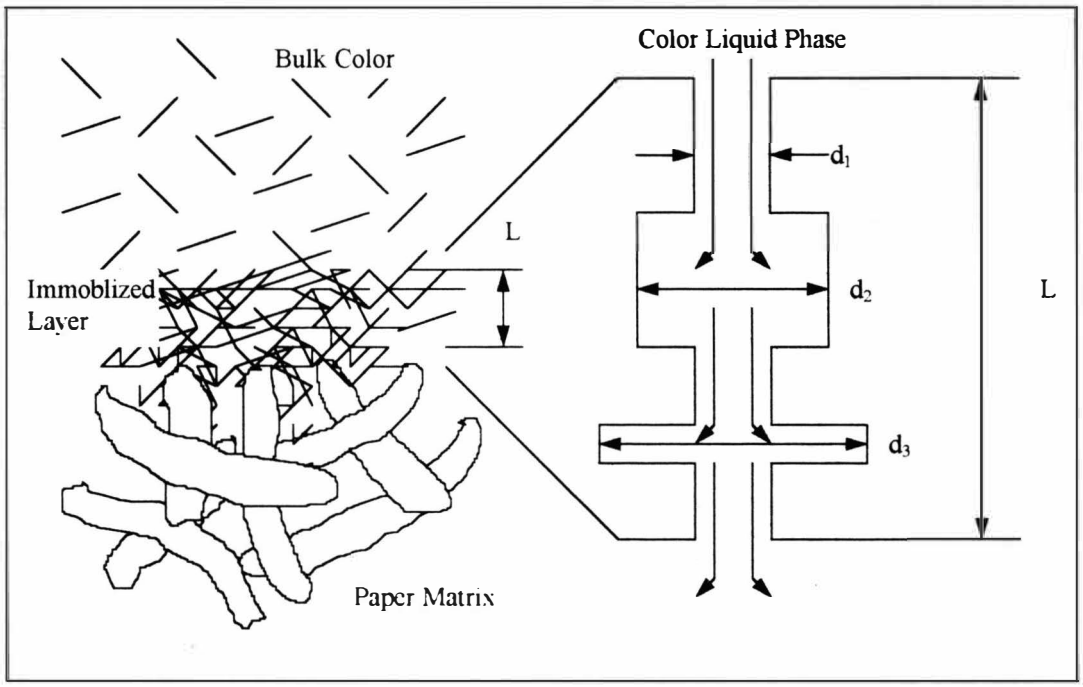

Figure 10. Schematic View of Color Phase Interface and Pore Model (11).

The capillary migration can be slowed by increasing the water viscosity with addition of a water soluble polymeric thickener or co-binder and sometimes by a change in the binder surfactant which would reduce the paper wetting. The water loss due to pressure migration may conceivably be reduced by reducing the driving force (blade pressure), increasing the water viscosity by adding thickener or cobinder, or by increasing the coating solids to reduce available water and reduce flow pathways(14). The platy pigments, which tend to be closely packed in the direction parallel to the flow field under the blade, may cause added tortuosity to resist the passage of fluid under pressure. Once a filter cake is formed, the flowing water has to move through an additional porous medium which has much smaller pore openings than the paper medium(15). Thus, filter cake formation should substantially reduce subsequent water migration (Figure 10).

Coating water retention can be strongly influenced by interactions between the water soluble polymeric thickener and clays. For clay-absorbing cellulosic thickeners, which tend to cause more structure building and faster immobilization, the cake formation mechanism appears to play major role in limiting water loss.

1.3.2 Coating Rheology

Coating colors are known to be complex systems containing mineral pigments, dispersant, binders, water retention aids and also minor amount of other additives in which interaction occurs. Coating colors have traditionally been described as a continuous fluid, having a well-defined macro rheology derived from micro interaction between pigment

color should be free from macroscopic contaminants, such as extraneous paper fibers, debris, aeration, oversize mineral particles. It should not be subjected to de-stabilization through the chemical invasion, ionic concentration, etc. The measurement of the viscous component at above type color, at varying shear rate and extended time scales provided the norm for coating color characterization(15).

Generally, continuous single phase systems behaves as a Newtonian fluid and the shear stress is related to shear gradient as follows,

$$\sigma = \eta\gamma$$

where σ is the shear stress, η is the viscosity and γ is the shear rate.

In the case of Newtonian fluids, viscosity do not change with the shear rate and the time of shearing. When the shearing is stopped, immediately the stress in the liquid falls to zero. The viscosity changes only with change in pressure and temperature(16). Coating formulations are two phase systems, being an aqueous-solid suspension. Two phase systems like coating colors exhibit very interesting shear and time dependent rheology(17).

1.3.2.1 Shear Dependent Phenomena. The viscosity of these materials has been studied over a wide range of shear and it was observed almost all the coating material take the shape of curve.

At low shear, the coating colors flow as Newtonian fluids of very high viscosity. As the shear rate increases, shear thinning behavior is observed where viscosity decreases with the increase in shear rate. The theories of shear thinning postulate that the dispersion

at rest forms a structure, which is broken down by the shearing forces and hence reduction of the viscosity is observed, as shown in Figure 11. It is called shear thinning or pseudo plasticity. When a shear thinning liquid is subjected to a transient jump in the shear rate, the system will relax to that degree of structure which corresponds to the new shear rate. At higher shear rates, the viscosity is again found to be constant and this zone is described as high shear Newtonian Zone. When shear rate is further increased, viscosity starts increasing. This is believed to be because in high shear Newtonian zone particles are organized normal to the velocity gradient, but as shear rates increases, this structure collapses and particles start sliding over adjacent layers. Under these circumstances, the resistance to flow increases to the extent that the fluid starts behaving like a solid. Shear blocking is observed and viscosity rises with shear rate. This behavior is called dilatancy(17).

1.3.2.2 Time Dependent Phenomenon. It is type of the hysteresis loop between increasing shear rate (up) and the decreasing shear rate (down) curves. If viscosity is higher in the up loop than down loop, it is called thixotropy. When viscosity is lower in the up loop than down loop, it is called anti-thixotropy. This behavior is due to a breakdown in structure (Figure 12 and Figure 13).

At low shear rate, the coating color may exhibit viscoelastic behavior. The interaction between pigment particles and particles with the component in the continuous phase forms a network structure which causes the viscoselastic nature of coating. It plays

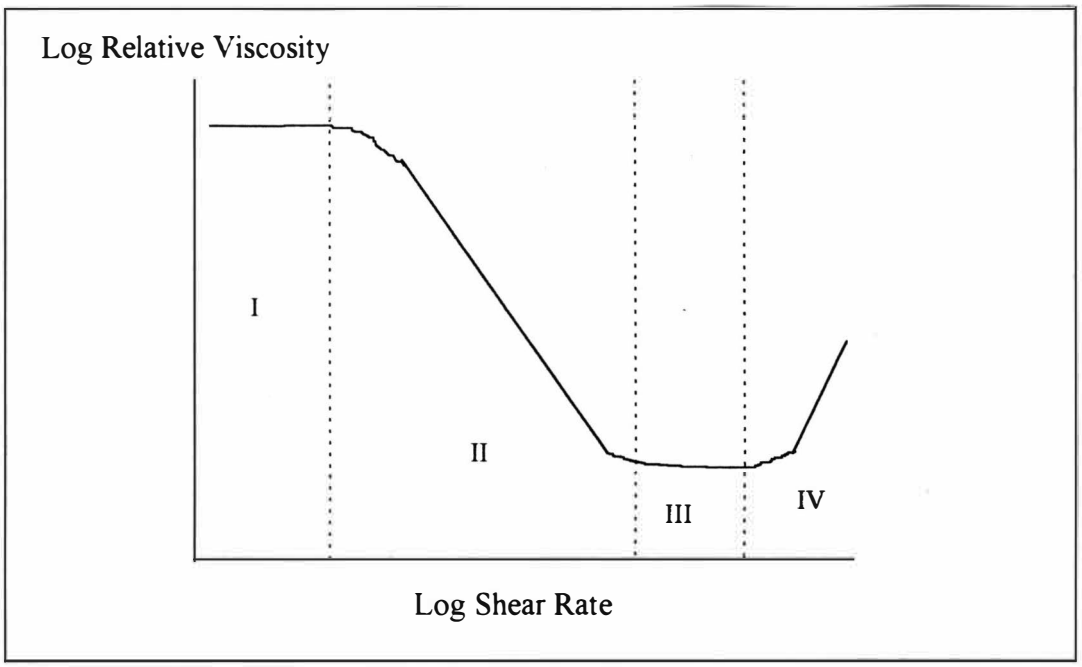

Figure 11. Schematic Graph Showing the Four Flow Regimes (21).

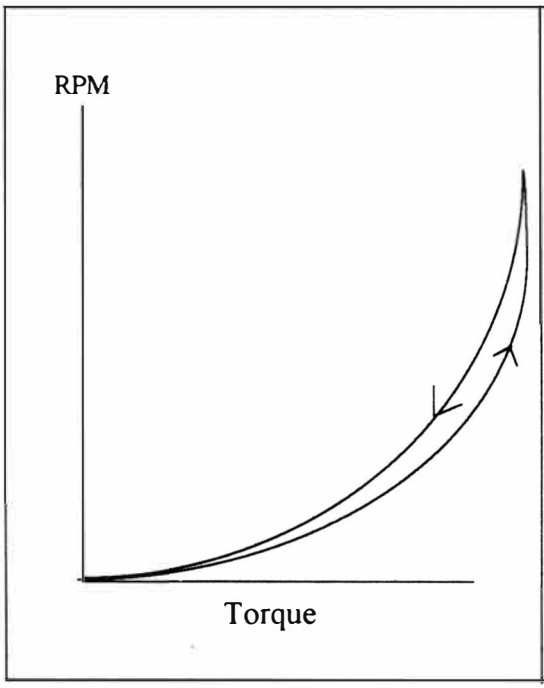

Figure 12. Thixotropy (26).

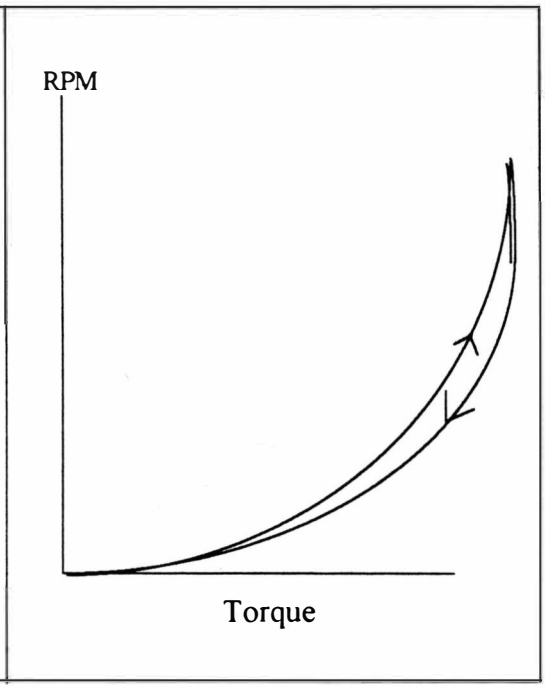

Figure 13. Anti Thixotropy (26).

an important role in the zones of low shear, as in the flow of coating prior to metering and after the exit from the blade tip. Viscoelasticity prevails during consolidation of the wet coating deposited on the substrate(18). However, the elastic behavior is minimized at high shear rate because the structures are sensitive to shear and cease to exist at high shear rates(19).

2. Forces in Bevelled Blade Coating

In blade coating, the coat weight or coating thickness passing between blade tip and base paper is determined by the balance of the forces acting on the blade and paper. These forces are both external and dynamic(20).

2.1 Tube Pressure

This is external mechanical force applied by the tube on the blade to regulate the coat weight. It also presses the bevel edge against the paper and backing roll and resists the dynamic forces generated due to the movement of web and coating color which tries to lift the blade.

The actual blade tip force can be calculated by the following equation,

$$F_Z = \left[1 + \frac{1}{2}\left(\frac{X_1}{X_2}\right)^3 - \frac{3}{2}\frac{X_1}{X_2} \right] F + 3D\frac{W}{X_2^{\,3}}$$

where X_1 and X_2 are blade dimensions, W is the deflection of the blade tip, and D is the stiffness index of the blade. The stiffness index D can be calculated by,

$$\frac{Ed^3}{12(1-\nu)^2}$$

where E is the Young's modulus of elasticity, d is the blade thickness, and υ is the material factor, having the value 0.3 for steel.

The force perpendicular to the base can be obtained by,

$$F_0 = F_Z . \cos \alpha$$

where α is the blade angle.

From the above equation, it is clear that the external mechanical force depends on the material, blade extension from the hose, blade thickness, and the deflection of the blade tip.

2.2 Dynamic Forces

During coating, excess color is transferred by the applicator roll to the web. The coating color strikes against the blade and excess color is metered by the blade. The excess color changes its direction and flows down the blade. Some of the coating color passes underneath the blade and gives the final coat weight.

During this whole operation three dynamic forces are generated.

2.2.1 Pressure Force

When coating enters in the wedge shaped space between blade and paper, it causes local alterations in color velocity. So a speed induced force arises. (see Figure 14.)

An expression for this pressure force can be derived by using potential theory and Bernoulli equation inside the control volume.

For flow that is considered non frictional and nonturbulent (2) we get

$$P_z = \frac{1}{2} m U_1 \frac{\pi}{\alpha}\left[1-\left(\frac{1}{2}-\frac{1}{\pi}\right)\frac{h_0}{h_2}\right]\left[1-\frac{1}{\left(2\frac{\pi}{\alpha}-1\right)}\left(\frac{1}{1-\left(\frac{1}{2}-\frac{1}{\pi}\right)\frac{h_0}{h_1}}\right)^2\right]$$

where h_0 is the thickness of coating color passing under the blade tip, h_2 is the thickness of coating color reaching the blade, $\dot{m}$ is the mass flow doctored by the blade, U_1 is the velocity of paper, and α is the blade angle (Figure 15).

This force decreases as the angle alpha is increased. This force is directly proportional to the product of mass flow and velocity.

2.2.2 Impulse Force

This force originates due to the change in the momentum of excess coating doctored off by the blade. When the excess coating color strikes the blade, its direction changes. These forces conserve the momentum in the arbitrary selected volume near the

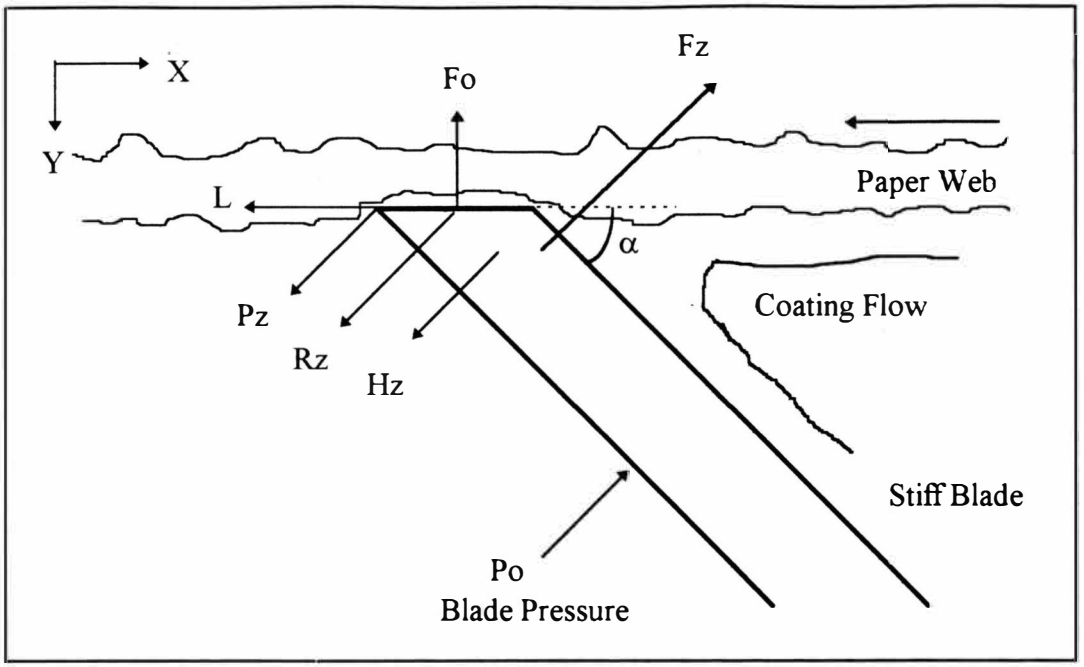

Figure 14. Blade Pressure Transmission to the Paper (12).

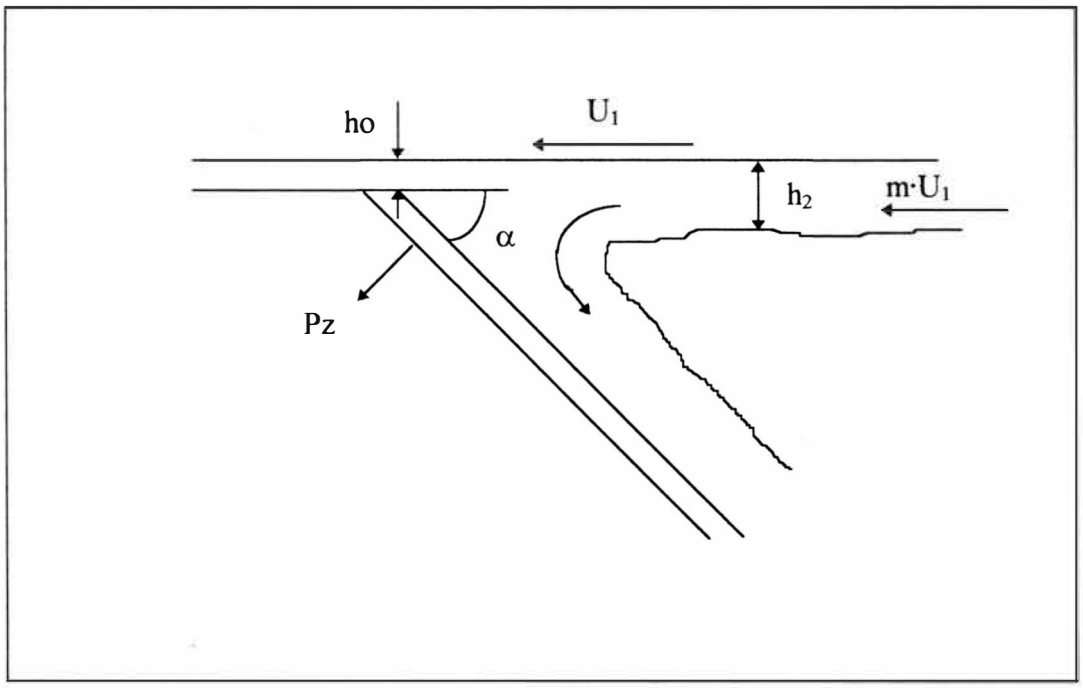

Figure 15. Pressure Force Pz Acting on the Blade (12).

blade heel. If we disregard the frictional losses and if the velocity of coating mass is considered to be constant, the impulse force can be calculated by following equation (21),

$$R_z = m \cdot U_1 (1 + \cos\alpha) \sin\alpha$$

where m is the mass flow doctored by the blade, U_1 is the velocity of color (paper speed), and α is the blade angle.

This force works perpendicular to the blade (Figure 16).

R_z is reduced as the blade angle is reduced and it is also directly proportional to the product of mass flow rate and velocity.

2.2.3 Hydrodynamic Force

This force is generated by the lubrication flow in the channel between the tip of the blade and surface of the paper. Turai has also considered that this force develops when liquids get into the wedge shaped nip(21). There is large velocity difference between the blade surface and liquid phase (Figure 17).

The fundamental assumption in lubrication analysis of blade coating is that two dimensional flow field is represented by one dimensional flow field in which pressure is a function of the downstream coordinate(x) only(21). Although many people have considered the flow in the blade nip as the converging channel, others have simplified it as parallel channel, formed due to web compressibility and blade wear. Turai analyzed beveled blade coating based on the concept of development of the pressure gradient similar to a

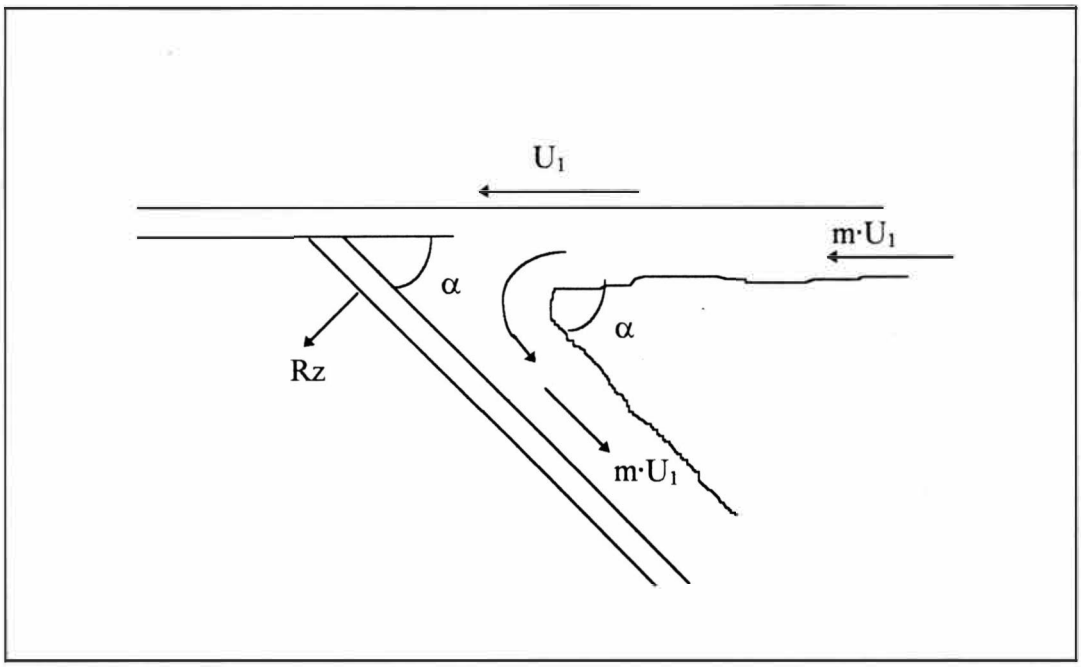

Figure 16. Impulse Force Rz Acting on the Blade (12).

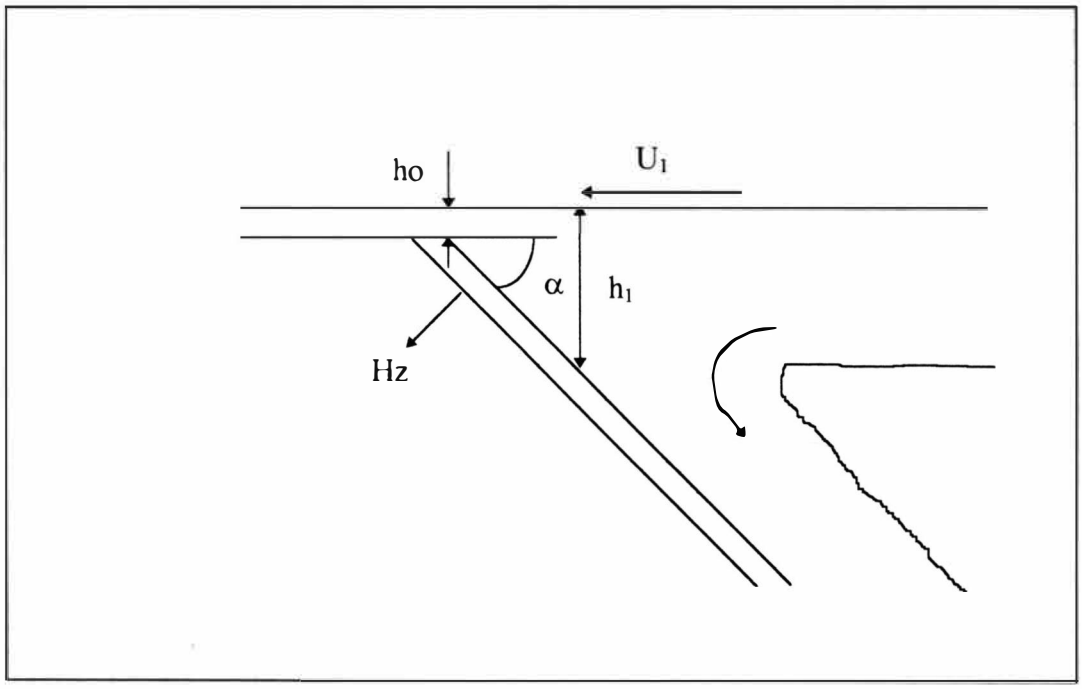

Figure 17. Hydrodynamic Force Hz Acting on the Blade (12).

journal bearing. In the case of a parallel channel flow, a pressure gradient presumably exists prior to the nip entrance due to the converging flow, approaching the nip. The gradient disappears inside the nip, so that flow can be characterized by simple shear. Turai has considered the flow as laminar between two parallel straight walls. He pointed out that when liquid gets into the wedge shaped structure, the viscosity of liquid becomes an influencing factor and a viscosity dependent hydrodynamic pressure in the coating may be experienced in the close proximity to the blade edge, where the coating color no longer flows down along the blade. The hydrodynamic force will cause a perpendicular pressure against blade and can be calculated from following equation,

$$H = \frac{6\mu\left(\frac{t}{Sin\alpha}\right)^2}{h^2}\left(1-\frac{2h_w}{h}\right)$$

where t is the blade thickness, h is the blade nip gap, and h_w is the final wet film thickness.

In actual coating process, under stable operating conditions, paper compressibility and roughness control the coat weight pickup. Based on this concept, Kahila and Eklund developed a theory based on the impact of the excess coating layer at the underside of the blade upstream of the blade nip entrance(21). Under equilibrium, the tip of the blade can be considered parallel to the web surface, so that no hydrodynamic lubrication force is accounted for inside the blade nip. Triantafillopoulos has stated that because of this, the hydrodynamic lubrication force will be close to the blade entrance at the location where coating no longer flows down along the blade, but deflected away from the blade nip.

The equation for it can be given by(21)

$$H_Z = \frac{6\eta U_1}{\tan^2 \alpha}\left[\ln(1+m) - \frac{2m}{2+m}\right]$$

where η is the viscosity.

$m = h_1/h_0 - 1$

Where h_1 is the distance between blade and base at the point origin of the pressure and h_0 is the distance between blade and base at the blade tip.

CHAPTER III

PROBLEM STATEMENT AND OBJECTIVES

The two phase-systems in coatings has been a subject of interest for coating colors and its behavior on coating applications. The coating formulations are dispersions, which include solid particles dispersed in a liquid phase. The presence of a dispersed phase increases the viscosity of coating colors. The measured viscosity of color is viewed as the sum of the viscosity of the continuous phase and incremental increase in the viscosity due the addition of the solids or dispersed phase. At low shear rate, the effect of the continuous phase on viscosity is found to dominate but at high shear rate, the dispersed phase dominates.

Different researchers have different conclusions about the relative importance of viscosity on blade forces. Most have not measured the actual blade force, but only computed it based on indirect measurement. Guler and Bousfield have developed a new technique to measure the blade forces by measuring the deflection of the beveled blade(22). by mounting a position detector on the bottom side of a laboratory puddle coater. The blade position is recorded by a computer every millisecond. From the blade deflection and a calibration step, the actual forces are known. They compared experimental blade forces with a model based on lubrication theory and found that experimental forces are larger than

the forces which are calculated by lubrication model. They also observed that viscoelastic fluids gave lower blade forces compared to viscous fluids.

In this study the main objective is to find the effect of two phase systems on blade forces in beveled blade coating by measuring the blade deflection. Two coating colors at 40% solids, 55% solids and a polymer solution at 0% solids of similar high viscosity have been used. The formulations were coated on polyester film by using a Cylindrical Laboratory Coater. By analyzing the data, it can be implied to what extent presence of the dispersed phase affects the blade forces. If coating colors and polymer solution generate similar deflection, then it can be concluded that two phase system does not have significant effect on blade forces.

The other objectives are as follows,

1. To study the effect of increasing % solids of the coating formulations while maintaining the similar high shear viscosity.

2. To determine the importance of high shear viscosity on blade force.

CHAPTER IV

EXPERIMENTAL METHODS

1. Determination of Coating Rheology

1.1 Brookfield Viscometer

In this equipment, torque is measured from the revolving spindle in the coating reservoir. It is used to measure the viscosity at a low shear rate. The viscosity was measured by at #3 spindle at 100 rpm. Actually all the equipments measures kinematic viscosity which is referred as viscosity in this report.

1.2 Hercules Viscometer

In this type of viscometer, concentric cylinders with well-defined geometry are used. The gap between the rotating inner (bob) and the restrained outer (cup) cylinder is very small. It results in an approximately velocity-driven (Couette) flow, which is similar to the flow between two parallel plates, where one plate moves relative to other. It can measure viscosity up to 50000 sec^{-1} shear rate. The rotation of the bob causes the fluid to flow. The resistance of the fluid for deformation causes a shear stress on the inner wall of the cup which is measured in dynes/ cm^2. The viscosity is calculated by the computer attached with the equipment.

1.3 Eklund Capillary Viscometer

This equipment was used for measuring the viscosity at high shear rate up to the range of 10^6 sec^{-1}. Three capillaries were used of the sizes (1) 0.51 mm dia, 50.0 mm length; (2) 0.51 mm dia; 100.0 mm length; and (3) 0.66 mm dia and 100.0 mm length. The viscosity data was corrected for the Hagenbach and Rabinowitch correction factors.

2. Determination of Blade Deflection and Blade Force

2.1 Cylindrical Laboratory Coater

For conducting the experiments, a Cylindrical Laboratory Coater (CLC) was used. It is a high speed coater capable of stiff beveled blade coating up to 6000 feet per minute. The CLC uses a puddle applicator. It has three major units.

2.1.1 Coating Drum

It is a soft rubber coated drum on which paper or polyester film is wrapped for coating.

2.1.2 Coating Pond

The coating color is poured inside the pond. It has a stiff beveled blade at 50 degree contact angle. It is mounted on the pond carriage that is rapidly moved towards the drum during the coating operation and moves away from it once a coating cycle is

completed. The pond carriage moves across the drum face during the coating operation giving a helical coating pattern. During coating the pond supplies the excess coating on the paper and collects the coating color metered by the blade.

The term "Blade run-in", is used to indicate the gap between the bevelled blade and coating drum. One blade run is equal to 1/1000 inch. The higher the blade run-in, the smaller is the gap between the coating coating drum and bevelled blade. That is, at a blade run-in of 20, bevelled blade will be closer to the coating drum than at a blade run-in of 5. In our experiment for each coating, CLC runs were made at blade run-in of 5, 10, 15 and 20.

2.1.3 Infrared Drying Unit

The drying unit is mounted on the top of safety cover which is used to close the drum during coating. It has electric IR drying lamps and is covered by air driven shutters. These shutters open when lamps reach the desired temperature. For this experiment, drying is not done. All the samples were collected within 6 to 7 minutes after the CLC run for coat weight.

2.2 Blade Deflection Measurement

For measuring the deflection, a position detector (TESA SA, Tesatronic TTD20) was used. The similar unit was used by Guler and Bousfield (22) for measuring the blade deflection. A probe holder as shown in Figure 18, was mounted underneath the pond carriage. It can be clamped on the pond carriage by tightening the screw and can be

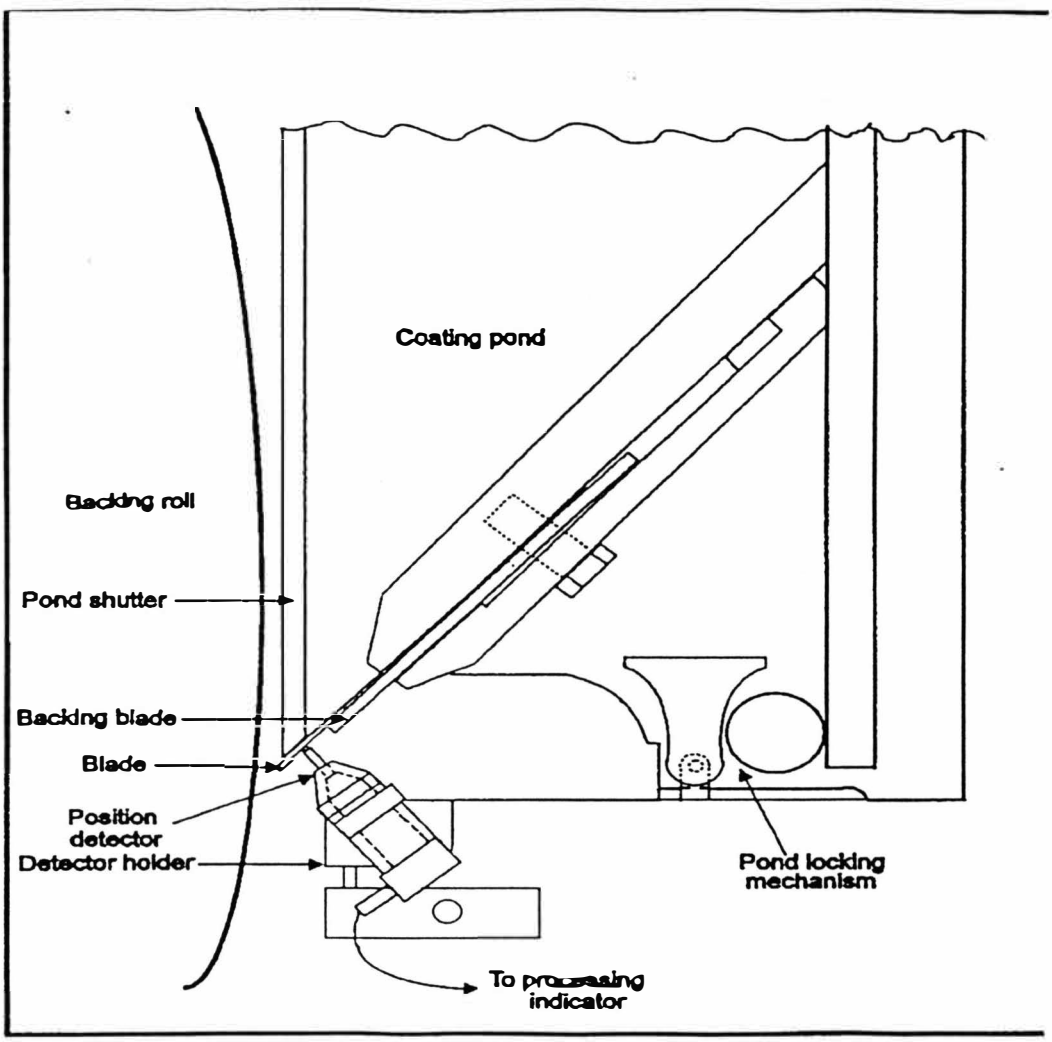

Figure 18. The CLC Pond With Position Detector(18).

removed easily whenever required. The position detector was mounted on the probe holder. A metering device was also attached to the holder so that the position of the probe with respect to the blade could be adjusted (Refer Figure 19, 20, 21). The probe, which has a spring loaded pin, touches the back side of stiff blade. During coating any deflection of the blade will cause a displacement in the pin of the probe. An amplifier was attached to the probe to amplify the signals of the probe and the voltage signals of the amplifier were sent to a computer for recording the data continuously (Refer to Appendix A for procedure).

2.3 Force-Deflection Calibration

The blade deflection corresponds directly to the probe deflection which is measured. Blade forces can be determined from a calibration plot between the probe deflection and the force applied to the blade. For making a calibration plot, a T shaped device (Figure 22) was used to generate controlled loading on the blade. It was mounted on the blade and a known force was applied to the blade. The probe measures the deflection of the blade for this known force. For another force, a different blade deflection was obtained. The data of the force and deflection were plotted and the slope of the line was then used to evaluate the blade forces during the coating operation (Figure. 32. Refer to Appendix A for procedure).

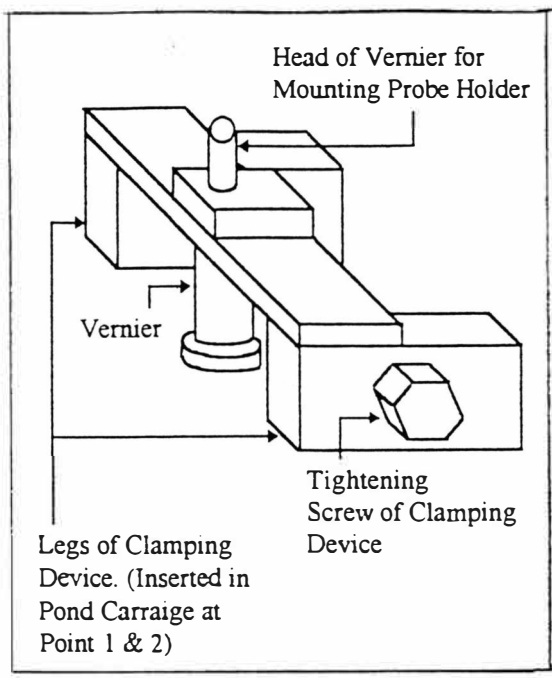

Figure 19. Pond Carraige.

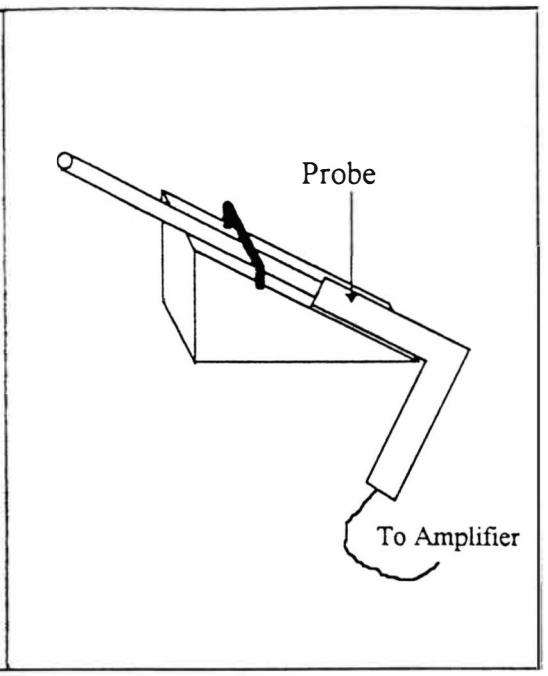

Figure 20. Probe Holder.

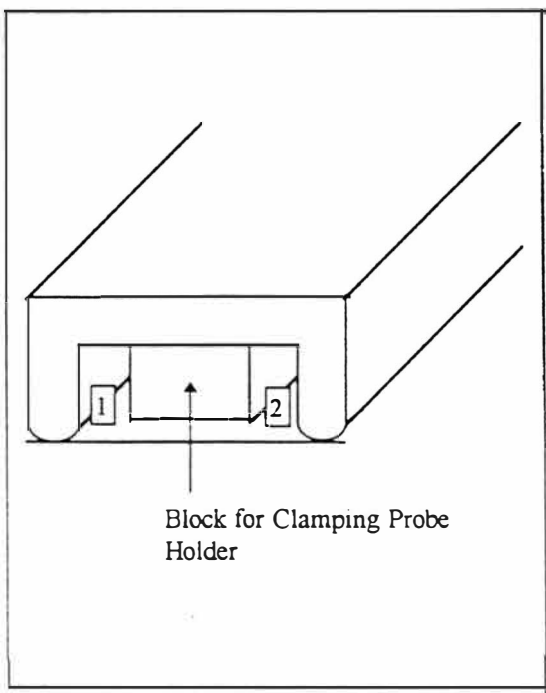

Figure 21. Clamping Device.

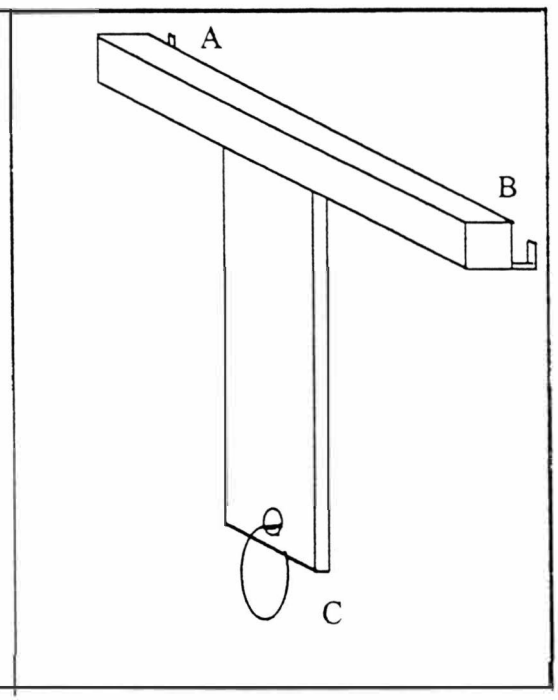

Figure 22. Calibration Device

3. Determination of Coat Weight

For this experiment, three coating colors at 0%, 40% and 55% solids were prepared as given in Tables 1 and 2. In Table 1 the actual weight of different coating components is given in grams. In Table 2, the percent quantity of the each coating component in coating formulation is mentioned. A Dow 620 latex, a DOW 720 plastic pigment and #2 clay were used. UCAR from Union Carbide was used as a viscosity modifier. The glycerin was supplied by Procter and Gamble. Dispex N-40 was used for the dispersion of #2 clay. The coating color at each % solids was prepared in three batches and they are mentioned as A, B, C. Each batch was prepared separately.

In this experiment, the coating was not dried with the infrared heater. The only water removal was due to the evaporation of water under atmospheric conditions. For determination of the coat weight, a sample was cut from the center of polyester film and its weight was taken within 5 minutes. After that, the sample was washed, dried, and weighed again. The coat weight was calculated as, (Wc-Wp)*Gp/Wc, where Gp, Wc, and Wp are the weight in grams per square meter of polyester film, weight of the coated sample, and weight of the polyester film, respectively.

In a separate experiment an approximate evaporation rate of the coating color was estimated for each coating and wet coat weight were corrected for the loss of moisture due to the evaporation of water (Refer to Appendix F).

Table 1

Coating Formulation

% Solids→	55	40	0
	(Weight of coating components in grams)		
#2 Clay (70% solids)	1782.9	1297.5	
Plastic Pigment (54.8% solids)	2279.0	1657.7	
Latex (50% solids)	506.7	368.5	
UCAR (26.0% solids)	20.4	99.2	285.0
Water	411.0	541	1315.0
Glycerin		1363.6	3400.0
Ammonia	8.2	1.1	25.0

Table 2

Composition of Coating Formulation on % Basis

% Solids→	55	40	0
#2 Clay (Dry basis)	24.92	17.01	0.00
Plastic Pigment (Dry basis)	24.93	17.01	0.00
Latex (Dry basis)	4.99	3.40	0.00
UCAR (Dry basis)	0.13	0.59	1.81
Water	44.87	36.23	30.03
Glycerin	0.00	25.54	67.66
Ammonia	0.16	0.21	0.50

CHAPTER V

RESULT AND DISCUSSION

1. Viscosity

1.1 Coating Formulation at 0% Solids

The Brookfield viscosity of all three batches at 0% Solids was in the range of 1200 to 1272 cp at 100 rpm. The coating formulations gave shear thinning behavior up to a shear rate of 1.5 X 10^6 sec^{-1}. The coating behaved as Newtonian fluid at shear rates higher than 1.6 X 10^6 sec^{-1}, and the viscosity values were around 12 centipoise. (Refer to Table 3. A, B, C represents three batches of 0% coating color.)

The viscosity data of all three coating colors were fit to the Cross Model (23) as given by

$$\eta = \eta_{\infty} + \frac{\eta_0}{(1 + k_1 * \gamma^n)}$$

where η is viscosity, η_{∞} is Newtonian viscosity at high shear rate, η_0 is Newtonian viscosity at low shear rate and K_1 and n are constants. For all three coating colors, the best curve fitting gave η_{∞} = 12, η_0 = 2200, K_1 = 0.0873, and n = 0.6099. The natural log of viscosity and natural log of shear rate were then plotted and it was observed that Cross

Table 3

Viscosity at 0% Solids

Run# →	7		1		5	
Coating→	0A		0B		0C	
S. No.	Shear rate Y (sec^{-1})	Viscosity η (cp)	Shear rate Y (sec^{-1})	Viscosity η (cp)	Shear rate Y (sec^{-1})	Viscosity η (cp)
1	2213444	12.2	1575662	15.3	2094975	13.0
2	1731970	12.2	1216917	17.3	1871029	12.4
3	962949	18.1	1051614	16.6	1639860	12.7
4	755647	18.6	858173	16.4	1134176	15.4
5	514910	20.7	597907	17.7	964411	14.6
6	325441	21.9	370468	19.2	754913	14.0
7	109223	32.7	152408	23.3	435851	16.3
8	46288	50.8	60670	29.3	187825	18.9
9	42080	54.1	46288	43.8	65016	27.5
10	37872	57.9	42080	46.2	46288	43.3
11	33664	62.1	37872	48.9	42080	46.0
12	29456	66.9	33664	52.0	37872	48.9
13	25248	72.4	29456	55.3	33664	52.2
14	21040	78.7	25248	59.2	29456	55.7
15	16832	87.2	21040	63.6	25248	59.6
16	12624	99.4	16832	69.8	21040	64.3
17	8416	118.4	12624	77.9	16832	70.6
18	4208	162.0	8416	91.7	12624	79.1
19	40	1200.0	4208	123.4	8416	93.9
20			40	1272.0	4208	124.3
21			10		40	1234.0

model fit all three coating formulation curves very well. In a regression analysis, for run number 7, 1 and 5 the R^2 value is found to be 0.99, 0.98 and 0.98 (Refer to Figure 23, 24 and 25). Since the fitted curve is same for all the three coating colors, it indicates that there was very little variability in the three coating colors at 0% solids.

1.2 Coating Formulation at 40% Solids

The low shear Brookfield viscosity of all three coating colors at 40 % solids had higher variability than 0% solids. The viscosity values were in the range of 1100 to 1300 cp. However, very consistent data were obtained from Hercules and Eklund viscometers. This coating had also shown the shear thinning behavior up to a shear rate of 800,000 sec^{-1}. At shear rates higher than this, it also behaved as a Newtonian fluid. The high shear viscosity appeared to be around 13 cp. The viscosity data of these coating colors was also fit to the Cross model as given in Table 4 and Figure 26, 27, and 28. The curve fitting gave $\eta_\infty = 13$, $\eta_0 = 1500$, $K_1 = 0.17818$, and $n = 0.58519$ as the best fit for all three coating colors at 40% solids. In a regression analysis, for run number 4, 2 and 9 the R^2 value is found to be 0.97, 0.98 and 0.97 (Refer to Figure 26, 27 and 28).

1.3 Coating Formulation at 55% Solids

All three coating colors at 55% Solids exhibited the lowest Brookfield viscosity, in comparison to 0% and 40% solids, of 950 to 1100 cp (Refer to Table 5. A, B, C represents three batches). This coating color also had shear thinning behavior approximately to a shear

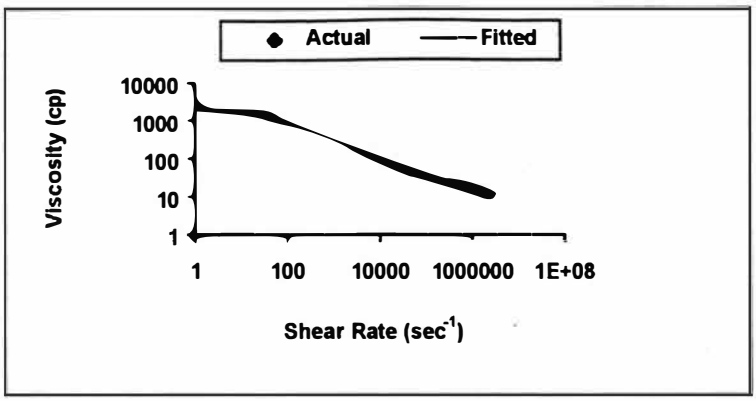

Figure 23. Viscosity Curve of Coating 0A.

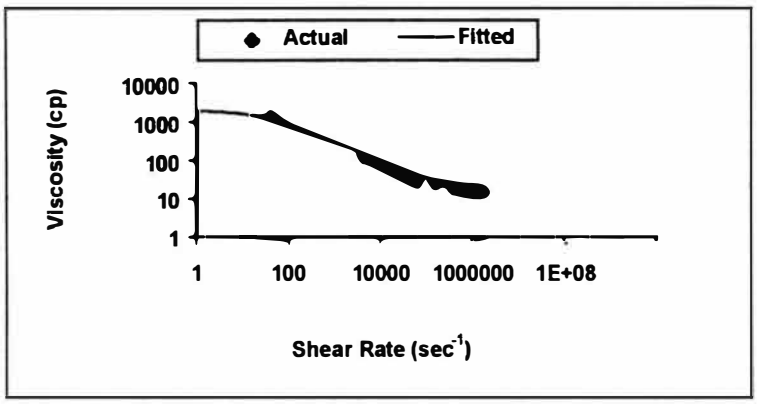

Figure 24. Viscosity Curve of Coating 0B.

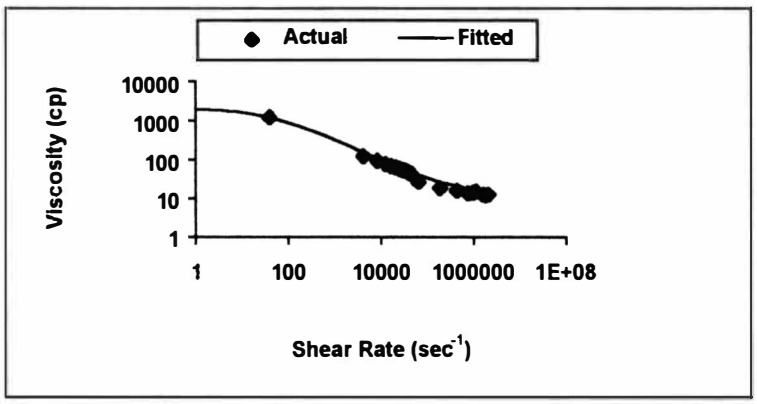

Figure 25. Viscosity Curve of Coating 0C.

Table 4

Viscosity at 40% Solids

Run# →	4		2		9	
Coating→	40A		40B		40C	
S. No.	Shear rate Y (sec^{-1})	Viscosity η (cp)	Shear rate Y (sec^{-1})	Viscosity η (cp)	Shear rate Y (sec^{-1})	Viscosity η (cp)
1	2050538	13.05	1797855	14.96	1825610	14.82
2	1534509	15.17	1459513	15.9	1494884	15.81
3	1222175	17.26	1333465	15.71	1501498	13.96
4	1028664	17.07	1031611	16.95	1031867	16.95
5	913237	15.34	955318	14.72	896269	15.77
6	675591	15.77	699903	15.04	707755	15.05
7	344020	20.91	426797	16.52	449788	15.79
8	190116	18.68	218927	16.14	229304	15.49
9	77235	22.88	97024	18.58	96737	18.27
10	46288	29.6	46288	29.3	46288	28.3
11	42080	30.7	42080	30.1	42080	28.9
12	37872	31.6	37872	31	37872	29.1
13	33664	32.3	33664	31.9	33664	29.6
14	29456	33.3	29456	33.1	29456	30.2
15	25248	34.5	25248	34.2	25248	31.2
16	21040	36	21040	35.6	21040	32.1
17	16832	37.9	16832	37.5	16832	33.6
18	12624	40.7	12624	40.8	12624	36.1
19	8416	46.1	8416	47	8416	41.4
20	4208	58.4	4208	61.7	4208	54.2
21	40	1112	40	1212	40	1314

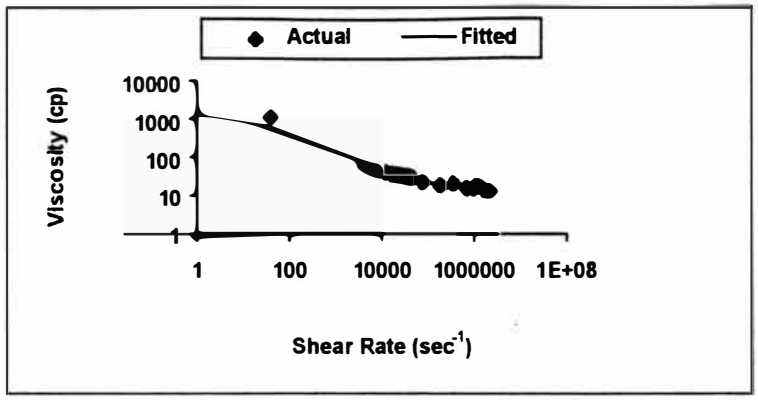

Figure 26. Viscosity Curve of Coating 40A.

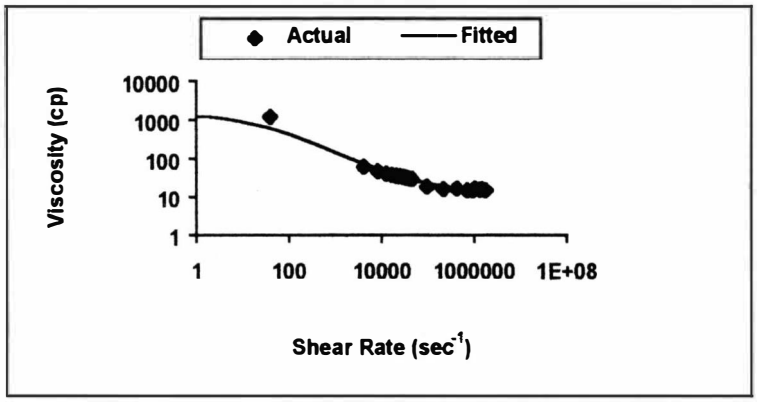

Figure 27. Viscosity Curve of Coating 40B.

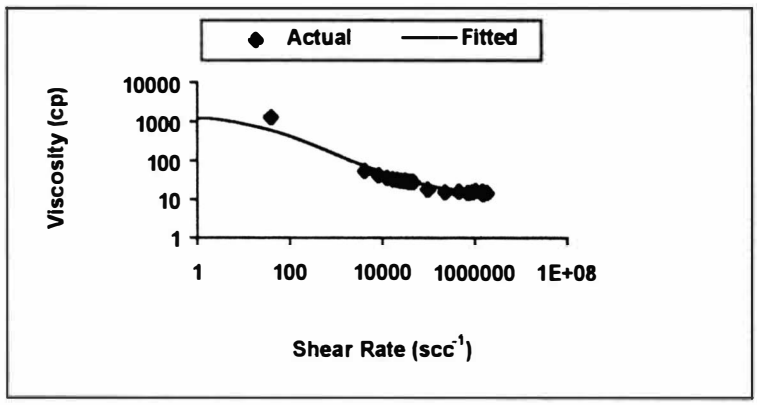

Figure 28. Viscosity Curve of Coating 40C.

Table 5

Viscosity at 55% Solids

Run# →	6		8		3	
Coating→	55A		55B		55C	
S. No.	Shear rate Y (sec^{-1})	Viscosity η (cp)	Shear rate Y (sec^{-1})	Viscosity η (cp)	Shear rate Y (sec^{-1})	Viscosity η (cp)
1	1780432	15.38	1853695	12.71	1845236	14.72
2	1474121	16.23	1045674	20.01	1627762	14.56
3	1499647	13.96	718901	19.66	1495939	13.6
4	1027418	17.04	686224	15.6	1054421	16.5
5	912551	15.45	550563	12.61	948979	14.89
6	743442	14.33	89120	10.01	767750	13.57
7	514772	13.76	46288	19.7	516227	13.62
8	293548	12.04	42080	20	285572	12.19
9	145179	12.29	37872	20.3	102971	17.51
10	65942	12.99	33664	20.2	46288	20
11	46288	20	29456	20.1	42080	20.3
12	42080	20.3	25248	20.2	37872	20.6
13	37872	20.5	21040	20.4	33664	20.3
14	33664	20.3	16832	21.2	29456	20.5
15	29456	20.5	12624	22.3	25248	20.9
16	25248	20.3	8416	26	21040	21.2
17	21040	21	4208	36.5	16832	22
18	16832	21.6	40	952	12624	23.4
19	12624	23.4			8416	27.1
20	8416	27			4208	37.6
21	4208	37.8			40	1104
22	40	998				

rate of 800,000 sec^{-1}. At higher shear rates, it showed shear thickening behavior. The viscosity in the shear range of 1 X 10^6 to 1.8 X 10^6 sec^{-1}, was higher by at least 4 to 5 centipoise than at 800, 000 sec^{-1} shear rate. The curve fitting is done for three coating colors at 55% solids based at Cross-Gillespie Model. The equation of this model takes into account the shear thickening behavior of coating formulations (23, 24).

$$\eta = \eta_\infty + \frac{\eta_0}{(1 + k_1 * \gamma^n)} + \frac{K_2 * \gamma}{(K_3 + \gamma)^2}$$

where η is viscosity, η_∞ is Newtonian viscosity at high shear rate, η_0 is Newtonian viscosity at low shear rate and, K_1, K_2, K_3 and n are constants. The constants, $\eta_\infty = 11$, $\eta_0 = 1500$, $K_1 = 0.06$, $n = 0.8$, $K_2 = 9.4$ X 108 and $K_3 = 1.6$ X 107 were selected by curve fitting. The natural log of viscosity and natural log of shear rate has been plotted and it was observed that all the three coating formulation curves are very close to the fitted curve. In a regression analysis, for run number 6, 8 and 3 the R^2 value is found to be 0.88, 0.85 and 0.90 (Refer to Figure 29, 30, and 31).

2. Coating Color Properties - Density and pH

1. All three coating colors at 0%, 40% and 55% solids had similar density. The densities at 0%, 40% and 55% solid were 1.16, 1.19 and 1.18 $grams/cm^3$ respectively. The maximum difference between densities was only 1.5% (Refer to Table 6).

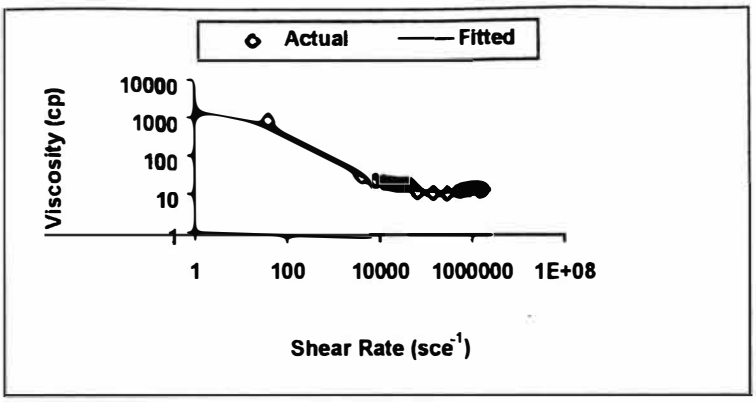

Figure 29. Viscosity Curve of Coating 55A.

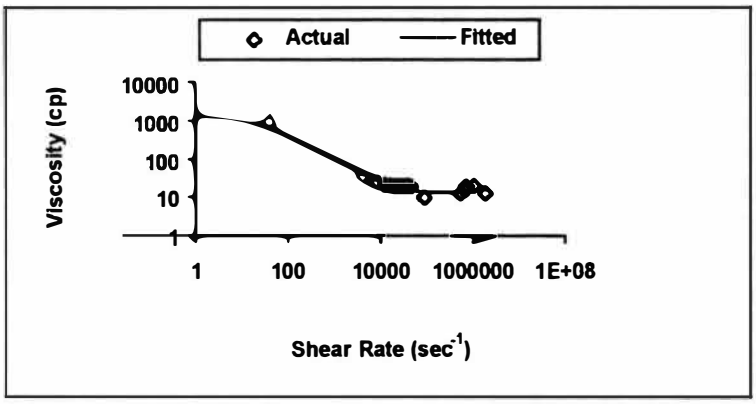

Figure 30. Viscosity Curve of Coating 55B.

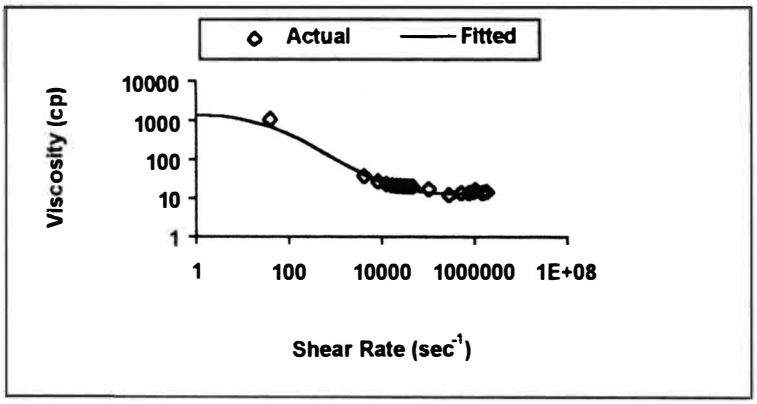

Figure 31. Viscosity Curve of Coating 55C.

Table 6

Coating Color Properties

Run#	Coating #	% Solids	Density gm/cm^3	pH	Temp ^{0}C	Brookfield 100rpm (cp)
1	0B	0	1.16	8.89	26	1272
2	40B	40	1.19	8.57	25	1212
3	55C	55	1.18	8.78	25	1104
4	40A	40	1.19	8.55	25	1112
5	0C	0	1.16	8.84	25	1234
6	55A	55	1.18	8.72	25	998
7	0A	0	1.16	8.53	25	1200
8	55B	55	1.18	8.83	26	952
9	40C	40	1.19	8.69	25	1314

3. Calibration of Deflection Measurement Unit

The calibration of blade force and blade deflection was done for each coating color to determine reliability in setup of carriage and probe unit. In nine sets of calibration data, the maximum coefficient of the variance was 3.9% at 5 Kg load. (Refer Table 7 and Figure 32). A graph between the average value of the blade deflection at each blade force (applied during the calibration) was plotted. A fitted line of the linear trend was also plotted. It was observed that the fitted linear deflection and actual graph of the deflection are almost overlapping. It shows that during the experiment there was linear relationship between the deflection of the blade and force applied on the blade.

Table 7

Calibration of Blade Deflection Measurement Unit

Run# → Load (Kg)	1	2	3	4	5	6	7	8	9	Average	%CV
	Blade Deflection in microns										
0.25	58	53	56	55	54	58	56	48	51	54	6.4
1	211	208	204	215	200	213	198	214	207	208	3.0
2	384	375	392	402	377	390	380	387	392	387	2.2
3	561	568	563	573	547	556	581	578	569	566	1.9
4	715	725	709	739	713	717	708	711	690	714	1.9
5	886	879	895	915	880	891	850	864	806	874	3.9

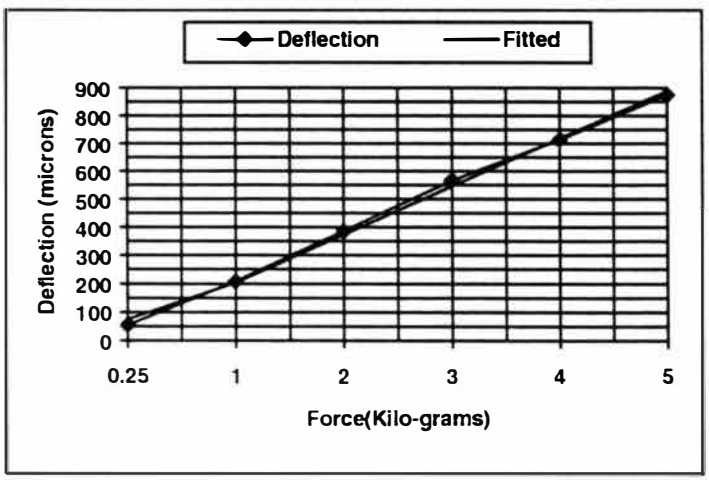

Figure 32. Calibration Plot.

4. Blade Deflection and Blade Forces

4.1 Experiment at 0% Solids

The coating colors at 0% solids were used in run numbers 1, 5 and 7 (Refer to Table 6). The average blade deflection at a blade run-in of 5 was 220 microns. As the blade run increased, blade deflection also increased. At a blade run-in of 10, 15 and 20, average average deflection was 308, 399 and 507 microns, respectively (Refer to Figure 33, 34 and 35). In these Figure, the deflection of blade vs time is plotted for each blade run-in and each run is slightly offset to reduce overlap. The time on the X axis is in sec/57, where 57 represents the frequency of data collection by the probe.). Since there is a linear relationship between blade deflection and blade force, the blade force has a similar trend. The average blade forces from the calibration plot, at blade run in of 5, 10, 15 and 20 were 1.1, 1.6, 2.1 and 2.7 kg respectively. The blade force increased as blade run-in increased. (Refer to Tables 8, 9, 10 and 11).

4.2 Experiment at 40% Solids

The coating colors at 40% solids were used in run numbers 2, 4 and 9 (Refer to Table 6). For 40% solids, a similar trend was observed. The average blade deflection increased as blade run-in increased. The data for the coating 40B at blade run in 20 was not collected, because the operator forgot to change the blade run-in. The average blade

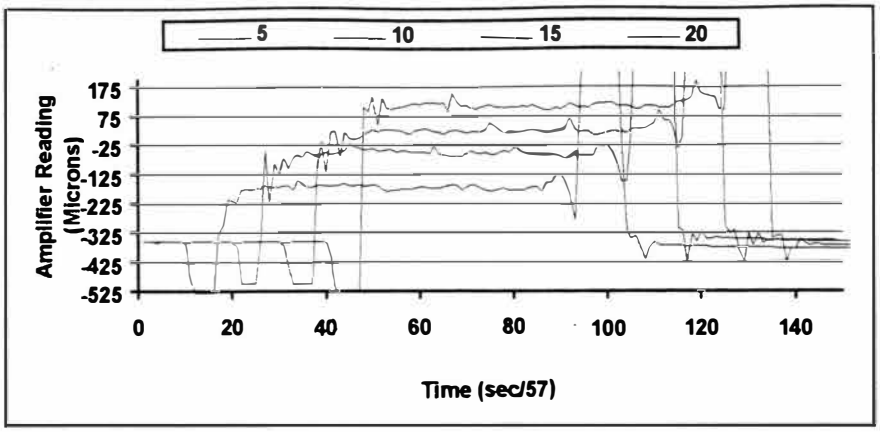

Figure 33. Blade Deflection of 0A.

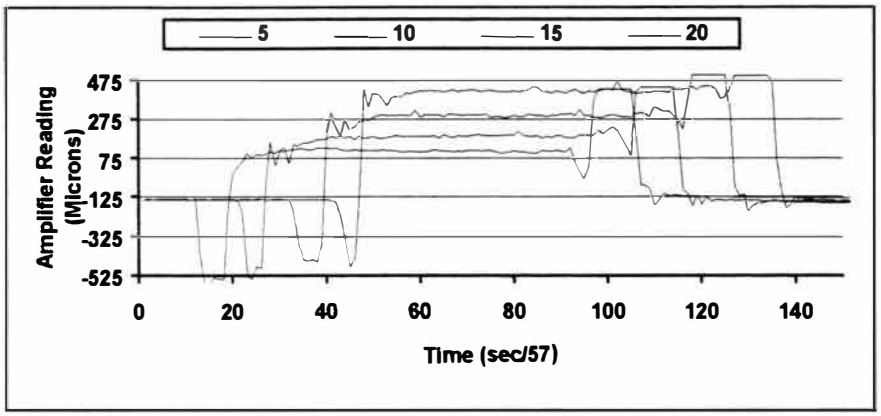

Figure 34. Blade Deflection of 0B.

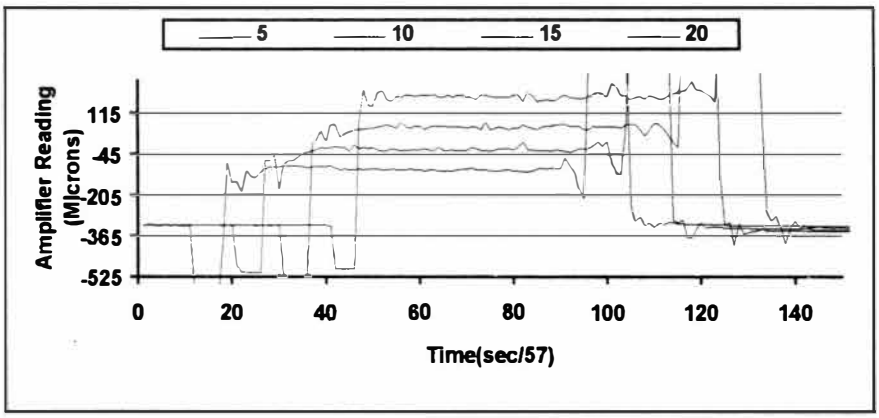

Figure 35. Blade Deflection of 0C.

Table 8

Blade Deflection in Microns

Blade Run in→	5			10			15			20		
	Deflection in Microns (microns)											
% Solids	A	B	C	A	B	C	A	B	C	A	B	C
0	186	251	222	303	324	298	378	433	386	462	556	503
40	186	226	144	266	295	245	372	395	306	521	399	433
55	149	111	146	243	205	264	325	306	360	454	411	542

Table 9

Average Data of Blade Deflection

Blade Run-in→	5		10		15		20	
	Avg (microns)	%CV	Avg (microns)	%CV	Avg (microns)	%CV	Avg (microns)	%CV
Coating 00	219.7	14.8	308.3	4.5	399.0	7.4	507.0	9.3
Coating 40	185.3	22.1	268.7	9.3	357.7	12.9	477.0	13.0
Coating 55	135.3	15.6	237.3	12.6	330.3	8.3	469.0	14.2

where Avg- Average, CV - Coefficient of variance (standard deviation * 100/Avg).

Table 10

Blade Force in Kilograms

Blade Run in→	5			10			15			20		
0% Solids	A	B	C	A	B	C	A	B	C	A	B	C
0	0.87	1.24	1.08	1.55	1.67	1.52	1.98	2.30	2.03	2.47	3.02	2.71
40	0.86	1.10	0.62	1.33	1.50	1.21	1.95	2.08	1.56	2.81	2.10	2.30
55	0.65	0.43	0.63	1.20	0.98	1.32	1.67	1.56	1.88	2.42	2.17	2.94

Table 11

Average Data of Blade Force

Blade Run-in→	5		10		15		20	
	Avg (Kg)	%CV	Avg (Kg)	%CV	Avg (Kg)	%CV	Avg (Kg)	%CV
Coating 00	1.1	17.7	1.6	5.2	2.1	8.2	2.7	10.0
Coating 40	0.9	27.6	1.3	10.8	1.9	14.5	2.6	14.3
Coating 55	0.6	21.3	1.2	14.8	1.7	9.6	2.5	15.5

Where Avg- Average, CV - Coefficient of variance (standard deviation * 100/Avg).

deflection at a blade run-in of 5, 10, 15, and 20 was 185, 269, 358, and 477 microns, respectively (Refer to Figures 36, 37 and 38). The blade force at a blade run-in of 5, 10, 15, and 20 was 0.9, 1.3, 1.9, and 2.6 Kilograms respectively. (Refer to Tables 8, 9, 10, and 11).

4.3 Experiment at 55% Solids

The coating colors at 55% solids were used in run numbers 3, 6 and 8 (Refer to Table 6). The average blade deflection at a blade run-in of 5, 10, 15 and 20 was 135, 237, 330 and 469 microns, respectively. In this case, the blade deflection also increased with blade run-in. The average value of blade force at blade deflection 5, 10, 15 and 20 was 0.6, 1.2, 1.7 and 2.5 kilograms, respectively (Refer to Figures 39, 40 and 41 and Tables 8, 9, 10 and 11).

5. Coat Weight

It was very difficult to get the samples for the coat weight and as a result of this, all samples could not be collected. (Refer to Table 12 for missing data of coat weights.)

The coat weight of all the coating colors were maximum at a blade run-in of 5. As blade run-in was increased, the coat weight decreased. The coat weight of 0% solids was the highest, followed by 40% Solids. The 55% solids had the lowest coat weight in all the cases. The coat weight data was used in the calculation of the shear rate under the blade (Refer to Tables 12 and 13).

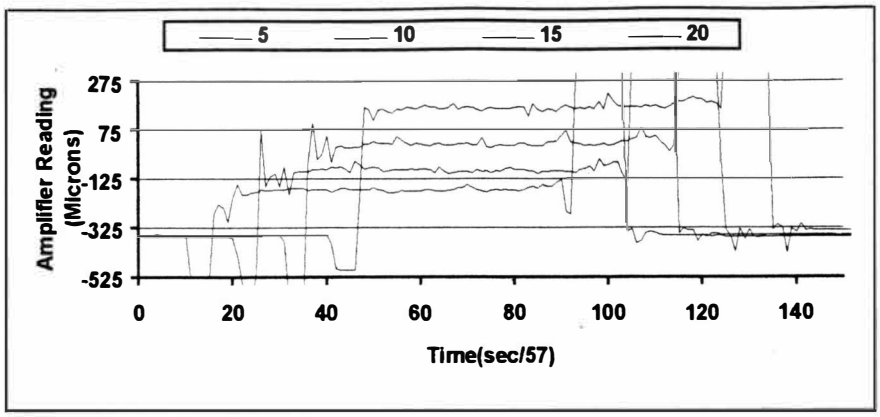

Figure 36. Blade Deflection of 40A.

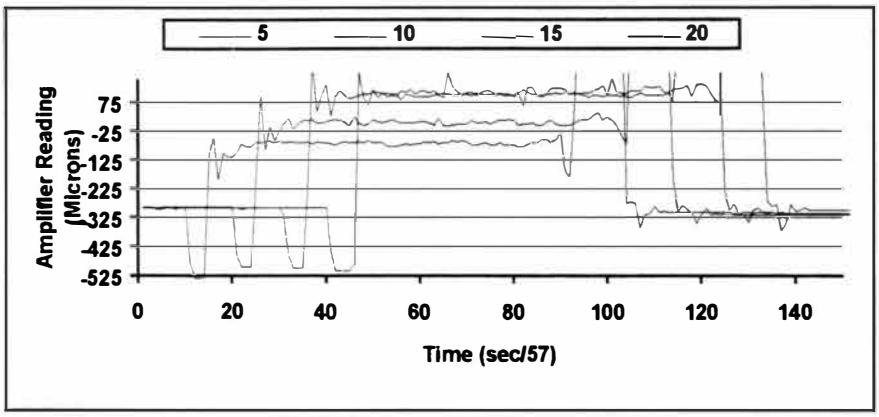

Figure 37. Blade Deflection of 40B.

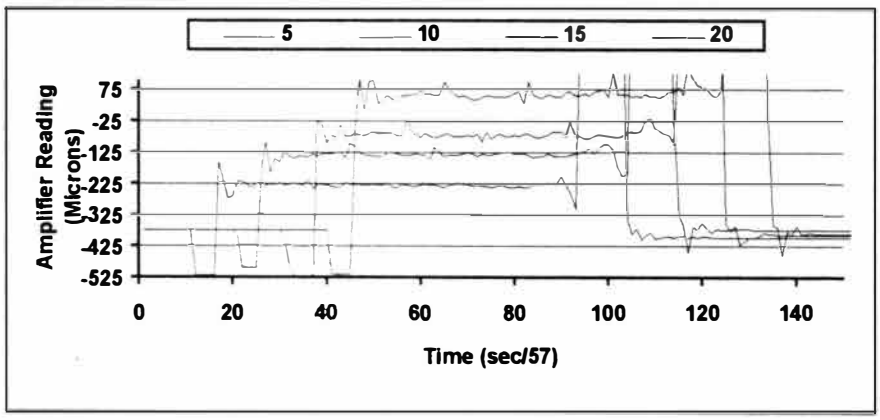

Figure 38. Blade Deflection of 40C.

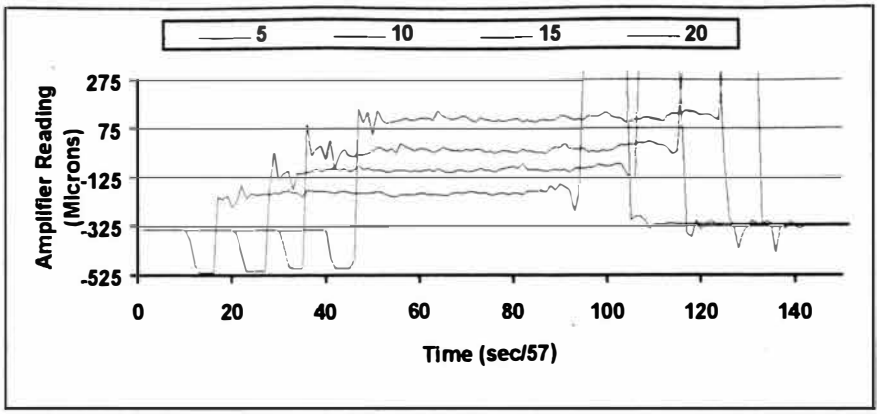

Figure 39. Blade Deflection of 55A.

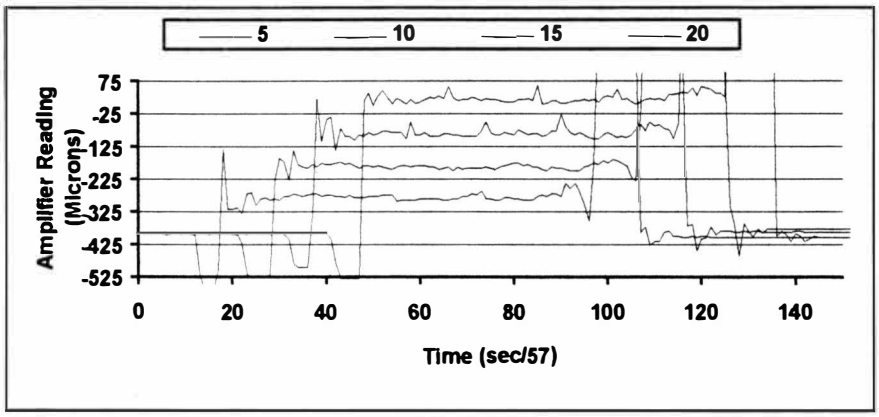

Figure 40. Blade Deflection of 55B.

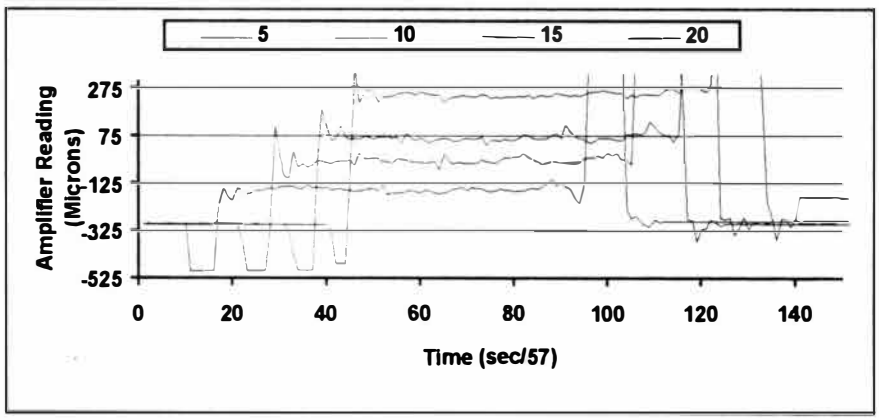

Figure 41. Blade Deflection of 55C.

Table 12

Coat Weight in Grams/Meter^2

Blade Run in→	5			10			15			20		
0% Solids	A	B	C	A	B	C	A	B	C	A	B	C
0		136	324			86	46	45	51	16	23	24
40	181	123	259	47	67	72	22	28	34	11		13
55	183	274	151	44	55	39	18	23	15	10	12	10

Table 13

Average Data of Coat Weight

Blade Run-in→	5	10	15	20
	grams/meter^2	grams/meter^2	grams/meter^2	grams/meter^2
Coating 00	230.0	86.0	47.3	21.0
Coating 40	187.7	62.0	28.0	12.0
Coating 55	202.7	46.0	18.7	10.7

6. Statistical Comparison of Coating Colors at 0%, 40%, 55% Solids

6.1 Design of the Experiment

In this experiment there were several factors that might have contributed to variability within the data.

1. There were different persons working during the experiment.

2. After a few runs, the blade started becoming very dirty and thorough cleaning and readjustment of blade was required.

3. Since the CLC room is not air-conditioned, atmospheric variation may have occurred, within the period of 8 hours.

4. The Polyester film may not be uniform in thickness or surface roughness.

To avoid variability associated with the above factors a "COMPLETE RANDOMIZED BLOCK DESIGN," for nine sets of experiments, was selected. The runs within the blocks were randomized (Refer Figure 42).

In this experiment, a block consists of the three CLC runs. Experiments were completed in three blocks. The three coatings at 0%, 40% and 55% solids were three treatments and the significance level was set at 5%, giving an α equal to 0.05. In Figure 42, the % solids are shown by 0, 40 and 55 and A, B and, C represents the batch number.

In one block, the same individuals were involved in the experiments and thorough cleaning of blade was not done. Blade setting was the same for all three runs and the time

Block 1	Block 2	Block 3
Run 1 Coating Color 0B	Run 4 Coating Color 40A	Run 7 Coating Color 0A
Run 2 Coating Color 40B	Run 5 Coating Color 0C	Run 8 Coating Color 55B
Run 3 Coating Color 55C	Run 6 Coating Color 55A	Run 9 Coating Color 40C

Figure 42. Distribution of Nine Runs Within Three Blocks.

period in one block was not big enough to expect significant changes in the atmospheric condition, or change in the polyester film.

6. 2Statistical Model

The statistical model for the design is

$$y_{ij} = m + t_i + b_j + e_{ij} \quad \{i \text{ (no of treatments)} = 1, 2, 3;\ j(\text{ no of blocks}) = 1, 2, 3\}$$

where m is an overall mean, t_i is the effect of the ith treatment, b_j is the effect in the jth block, and e_{ij} is the random error (25).

For the equality of the treatments, the hypothesis of interest will be

$$H_0 : m_1 = m_2 = m_3$$

It means that all the treatments (solids level) are equal and there is no effect due to the difference in the treatments (solids levels) at α significance level which indicates the %risk involved in rejecting the null hypothesis.

For the inequality of the treatments, the hypothesis of interest will be

$$H_1 : m_1 \neq m_2 \neq m_3$$

It means that all the treatments are not equal and there is significant evidence of the difference in the treatments.

The data on viscosity, blade deflection and blade force were analyzed statistically by doing Analysis of Variance for Complete Randomized Block Design with minitab 10.5.

6.3 Blade Run-in of 5

6.3.1 Viscosity

The shear rate and viscosity at the shear rate, calculated under the blade, is given in Tables 14 and 15. (Refer to Appendix B for the calculation of shear rate. In calculation simple shear rate is assumed.) The analysis of the variance of the viscosity data at blade run-in 5 gives a p value of 0.005. Since p is less than 0.05, the viscosity of all the three coating colors at 0%, 40%, and 55% solids is considered significantly different. The average viscosity at the 0%, 40%, and 55% solids is 41.1, 26 and 15.2 cp at the shear rate of 51242, 62689, and 58345 sec^{-1}, respectively .

Table 14

Shear Rate of Coating Colors Under the Blade

Blade Run in→	5	10	15	20
	Shear Rate in sec^{-1}			
0% Solids	51242	137042	250757	561219
40% Solids	62689	190090	420914	982133
55% Solids	58345	256209	620295	1071418

Table 15

Viscosity at the Shear Rate Under the Blade

Blade Run in→	5			10			15			20		
	Viscosity in cp											
% Solids	A	B	C	A	B	C	A	B	C	A	B	C
0	49.2	38.0	36.0	31.2	24.0	22.8	26.0	22.0	18.0	20.0	18.0	15.2
40	26.0	26.0	26.0	18.4	16.8	16.4	19.6	16.8	15.8	16.6	15.0	16.4
55	14.9	14.2	16.4	11.6	11.0	13.5	13.5	12.8	13.7	16.4	18.7	15.6

Table 16

Average Data of Viscosity Values

Blade Run-in→	5		10		15		20	
	Avg cp	%CV	Avg cp	%CV	Avg cp	%CV	Avg cp	%CV
Coating 00	41.1	17.3	26.0	17.5	22.0	18.2	17.7	13.6
Coating 40	26.0	0.0	17.2	6.2	17.4	11.3	16.0	5.4
Coating 55	15.2	7.4	12.0	10.8	13.3	3.5	16.9	9.5

where Avg - Average, CV - Coefficient of variance (Std deviation * 100/ Avg)

Table 17

Statistical Significance Effect of Coating Solids(0, 40 and 55%) on Different Properties at Various Level of Blade Run-in

Blade Run in→	5	10	15	20
		p value		
Viscosity	0.005	0.014	0.064	0.421
Deflection	0.004	0.005	0.015	0.447
Force	0.004	0.005	0.015	0.423

6.3.2 Blade Deflection

The data on blade deflection are presented in Table 9. The analysis of the variance of the blade deflection, at a blade run-in of 5 gives a p value of 0.004. Since it is less than 0.05, the blade deflection of all three coating colors at 0%, 40%, and 55% solids at a blade run-in of 5 is significantly different. The maximum deflection occurs at 0% solids, followed by 40% solids.

6.3.3 Blade Force

Since there is a linear relationship between blade force and blade deflection, blade forces give similar results. The p value for blade forces at a blade run-in of 5 is 0.004. It is less then 0.05, so the blade force exerted by all the three coating colors at 0%, 40%, and 55% solid, is different. The maximum blade force is at 0% solids followed by 40% solids.

6.4 Blade Run-in of 10

6.4.1 Viscosity

The p value at a blade run-in of 10 is 0.014, again less then 0.05. The viscosity of all three of the coating colors at 0%, 40%, and 55% solids is considered significantly different at a blade run-in of 10. The average viscosity at 0%, 40%, and 55% solids is 26.0, 17.2, and 12.0 cp, respectively.

6.4.2 Blade Deflection

At a blade run-in of 10, the p value is 0.005. Since it is less than 0.05, the blade deflection of all the three coating colors at 0%, 40%, and 55% solids at a blade run-in of 10 is different. The maximum deflection is at 0% solids, followed by 40% solids.

6.4.3 Blade Force

The p value for the blade forces at a blade run-in of 10 is also 0.005, which is less than 0.05. The blade force of all the three coating colors at 0%, 40%, and 55% solids is considered different. The maximum blade force is at 0% solids followed by 40% solids.

6.5 Blade Run-in of 15

6.5.1 Viscosity

The p value at a blade run-in of 15 is 0.064, that is more than 0.05. The viscosity of all the three coating colors at 0%, 40%, and 55% solids is the same at the 5% significance level. The average viscosity at the 0%, 40%, and 55% solids is 22.0, 17.4, and 13.3 cp respectively.

6.5.2 Blade Deflection

The p value is 0.015. Since it is still less than 0.05, the blade deflection of all the three coating colors at 0%, 40%, and 55% solids, at a blade run-in of 15, is considered

significantly different. The maximum blade deflection is at 0% solids, followed by 40% solids.

6.5.3 Blade Force

The p value for blade forces at a blade run-in of 15 is also 0.015 which is less than 0.05. The blade force of all the three coating colors at 0%, 40%, and 55% solids is considered significantly different. The maximum blade force is at 0% solids followed by 40% solids.

6.6 Blade Run-in of 20

6.6.1 Viscosity

The p value at a blade run-in of 20 is 0.421, which is certainly very high in comparison to 0.05. In this case , the null hypothesis can not be rejected and the viscosity of all the three coating colors at 0%, 40%, and 55% solids is the same. The average viscosity at the 0%, 40%, and 55% solids is 17.7, 16.0, and 16.9 cp respectively.

6.6.2 Blade Deflection

The analysis of the variance of the blade deflection, at a blade run-in of 20, indicates that the p value is 0.447. This is also higher than 0.05. For the blade deflection at

a blade run-in of 20, the null hypothesis can not be rejected. The blade deflection of three coating colors at 0%, 40% and 55% solids at a blade run-in of 20, is considered the same.

6.6.3 Blade Force

The p value for blade forces at a blade run-in of 20 is 0.423, which is higher than 0.05. There is no statistically significant evidence that there is difference in the blade forces exerted by all three coating colors at 0%, 40% and 55% solids.

CHAPTER VI

CONCLUSION

From the experiments, it can be inferred that the blade forces are dependent on the high shear viscosity of the coating color. At a blade run-in of 5, the maximum viscosity was at 0% solid, followed by the 40% solids. Blade forces also followed the same ordering, with 0% solids being the greatest and 55% solids the lowest. (Refer to Figure 43). The average blade force at 0%, 40% and 55% solids at a blade run-in of 5 was 1.1, 0.9, and 0.6, kg respectively.

At a blade run-in of 10, the difference in the viscosities of the colors was reduced, and the difference in the blade force was also reduced. Maximum viscosity and maximum blade force were at 0% solids followed by the 40% solids.

At a blade run-in of 15, although the viscosities of all the coating colors were same at 5% confidence level, the blade forces of all three coating colors were different from eachother. However, the difference in the blade forces was small in comparison to blade run-in of 5 and 10.

At a blade run-in of 20, the viscosities of all three coating colors were the same. Three coating colors had not shown any statistically significant difference in the blade deflection and the blade force (Refer to Figure 43).

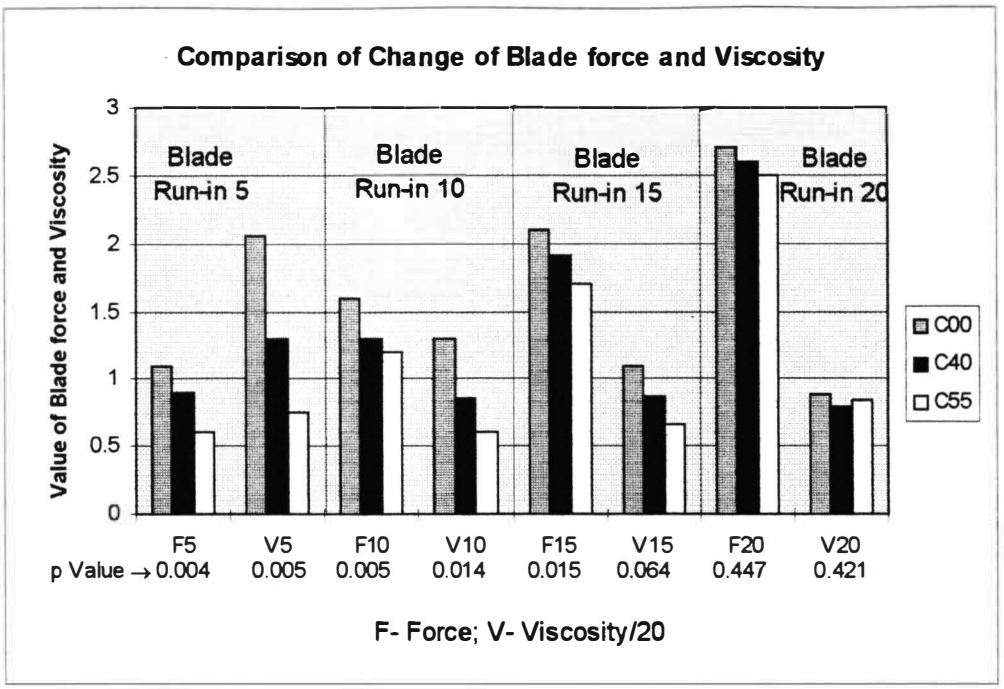

Figure 43. Comparison of Blade Force and Viscosity.

It was found that if the viscosity of single phase system and two phase systems is the same, then their effect on the blade forces will be the same. Therefore, if the rheological property of the two phase systems is similar to the single phase system, its behavior during the coating will be similar to the single phase system. Hence there should not be any significant difference in the blade deflection or blade force.

It can be concluded from this work, that if the viscosity of the coating color increases at high shear rate due to shear thickening behavior, it may significantly increase the blade force and a change in the coat weight will also be experienced. The other significant findings are as follows.

1.The blade deflection for each coating color increased with an increase in the blade run-in from 5 to 20.

2. The blade force and the blade deflection as measured in this work were found to have a linear relationship.

3. The 0% and 40% solids formulations showed the shear thinning behavior. However the coating at 55% solids was shear thinning up to 800000 sec^{-1} shear rate, with a shear thickening tendency at higher shear rates.

CHAPTER VII

RECOMMENDATION

Similar experiments can be conducted to evaluate the effect of paper roughness. For these experiments, coating colors of similar high shear viscosity and paper of different roughness can be used. A statistical analysis of the data of blade forces and paper roughness can be done to evaluate the effect of paper roughness on blade forces. The paper roughness should be measured at highest possible pressure permitted by the instrument in order to simulate the effect of paper compression on paper roughness during actual coating.

The effect of the water retention of coating colors on blade force may be of great interest. In this case same paper base can be coated with the coating colors of different water retention. For changing the water retention, different viscosity modifiers can be used, because it will not change the basic coating formulation. However, care should be taken to account for the significant change in the viscosity at higher shear rate. Usually these chemicals only affect the low shear viscosity. The data of blade forces and water retention can be analyzed to evaluate the effect of water retention on blade forces.

Appendix A

Procedure

1. Preparation of Coating Color

For the dispersion of the clay, a high shear clay disperser was used. For mixing the coating color, a coating mixer at low rpm was used.

1.1 Coating Color at 0% Solids

1. Glycerin was mixed with the water at low rpm.

2. UCAR was the added to mixture, at the same rpm.

3. Slowly ammonia was added to increase the pH. The speed of the mixer was adjusted to avoid the bubble formation. Above 7 pH whole the formulation started becoming very viscous and became transparent due to entanglement of the polymer chain. The final pH was adjusted to 9.

1.2 Coating Color at 40% solids

1. The #2Clay at 70% solids was prepared with high speed clay mixer and 0.05% dispex N40 was added in water before addition of clay.

2. Required amount of the clay and plastic pigment were mixed at low rpm.

3. Latex was then added and then Glycerin and water were also added.

4. After complete mixing, UCAR was added and the pH of the formulation was increased to 9 by ammonia.

1.3 Coating Color at 55% Solids

1. The #2 Clay at 70% was prepared with a high speed clay mixer and 0.05% dispex N-40 was mixed in water before addition of the clay.

2. Once the clay was completely dispersed, plastic pigment was added to it at low rpm.

3. Then latex was then added and then UCAR was also added. The pH of the coating color was increased to 9 with the help of ammonia.

2. Measurement of the Blade Forces

2.1 Fixing the Probe to the Pond Carriage

1. The probe was mounted on probe holder as shown in Fig 21. Then probe holder was mounted on the vernier of clamping device as shown in Fig 22.

2. As shown Fig 20, at position 1 and 2, two wooden pieces and two rubber padding were inserted in the pond carriage to avoid the movement of probe holder during the CLC run.

3. Then clamping device was inserted in the pond carriage at position 1 and 2, until it was blocked by the wooden pieces. Two wooden pieces had also been inserted at the top of the clamping device to prevent the vertical movement during the run of the CLC. The vertical position of the probe holder was checked with the help of anglemeter by placing it on the probe holder in vertical position. The anglemeter measures the angle from the horizontal plane. The screw in the clamping device has been tightened.

4. The probe was connected to the amplifier and the corresponding reading was noted. The tip of the probe was pressed to check the corresponding changes in the reading of amplifier. The change in the reading had assured the proper connections.

5. The pond was placed on the pond carriage and checked to ensure that the probe was in touch with the blade. The probe was moved to lowest position by rotating the knob on the vernier. At this point it was not touching the blade and a minimum reading was shown by amplifier. The probe was moved in upward direction by vernier and after some time the probe started touching the blade and there was change in the reading of the amplifier.

2.2 Calibration

1. For this purpose, a T shaped device was used as shown in Fig 19. The top portion was clamped to the blade with the help of C clamps at the position A and B.

2. The weight was hung at the hook and corresponding deflection reading was noted from the amplifier. Readings were taken for the weight of clamps and device and 1, 2, 3, 4 and 5 kg weight.

2.3 Measurement of the Blade Deflection During Run

The amplifier was connected to the computer. Then program 'PROBE_RUN' was run to collect the data as follows:

1. Start the 'PROBE_RUN' program and give necessary information.

2. Start the CLC with coating color and when the Infrared lamps turn red hit the "RETURN" key. The computer will started collecting the data. The pond will move and coating will be done. Once pond reaches to the other end of the CLC, hit the "RETURN" key in order to discontinue the data collection.

Appendix .B

Calculation of Shear Rate

For this simple shear condition has been assumed under the blade. The following is the formula for calculation.

Shear Rate = (Speed * Density * 10e+06)/Wet Coat weight.

Where unit for:

Shear Rate is 1/ sec

Speed is Meters /min (CLC Speed was 10.16 Meters/ min)

Density is gm/meter cube

Coat weight is grams per square meter.

Appendix C

Analysis of Blade Deflection

Blade Run-in 5

MTB > ANOVA 'Defl_5' = 'GroupNo' 'Coating'.

Analysis of Variance (Balanced Designs)

Factor	Type	Levels	Values
GroupNo	fixed	3	1 2 3
Coating	fixed	3	0 40 55

Analysis of Variance for Defl_5

Source	DF	SS	MS	F	P
GroupNo	2	5659.6	2829.8	15.80	0.013
Coating	2	10790.9	5395.4	30.12	0.004
Error	4	716.4	179.1		
Total	8	17166.9			

Blade Run-in 10

MTB > ANOVA 'Defl_10' = 'GroupNo' 'Coating'.

Analysis of Variance (Balanced Designs)

Factor	Type	Levels	Values
GroupNo	fixed	3	1 2 3
Coating	fixed	3	0 40 55

Analysis of Variance for Defl_10

Source	DF	SS	MS	F	P
GroupNo	2	2843.6	1421.8	9.70	0.029
Coating	2	7596.2	3798.1	25.91	0.005
Error	4	586.4	146.6		
Total	8	1 1026.2			

Blade Run-in 15

MTB > ANOVA 'Defl_15' = 'GroupNo' 'Coating'.

Analysis of Variance (Balanced Designs)

Factor	Type	Levels	Values
GroupNo	fixed	3	1 2 3
Coating	fixed	3	0 40 55

Analysis of Variance for Defl_15

Source	DF	SS	MS	F	P
GroupNo	2	6542.0	3271.0	13.17	0.017
Coating	2	7170.7	3585.3	14.44	0.015
Error	4	993.3	248.3		
Total	8	14706.0			

Blade Run-in 20

MTB > ANOVA 'Defl_20' = 'GroupNo' 'Coating'.

Analysis of Variance (Balanced Designs)

Factor	Type	Levels	Values
GroupNo	fixed	3	1 2 3
Coating	fixed	3	0 40 55

Analysis of Variance for Defl_20

Source	DF	SS	MS	F	P
GroupNo	2	12373	6186	5.09	0.080
Coating	2	2408	1204	0.99	0.447
Error	4	4859	1215		
Total	8	19640			

Appendix D

Analysis of Blade Force

Blade Run-in 5

MTB > ANOVA 'Force_5' = 'GroupNo' 'Coating'.

Analysis of Variance (Balanced Designs)

Factor	Type	Levels	Values
GroupNo	fixed	3	1 2 3
Coating	fixed	3	0 40 55

Analysis of Variance for Force_5

Source	DF	SS	MS	F	P
GroupNo	2	0.19130	0.09565	15.80	0.013
Coating	2	0.36475	0.18238	0.12	0.004
Error	4	0.02422	0.00605		
Total	8	0.58028			

Blade Run-in 10

MTB > ANOVA 'Force_10' = 'GroupNo' 'Coating'.

Analysis of Variance (Balanced Designs)

Factor	Type	Levels	Values
GroupNo	fixed	3	1 2 3
Coating	fixed	3	0 40 55

Analysis of Variance for Force_10

Source	DF	SS	MS	F	P
GroupNo	2	0.096118	0.048059	9.70	0.029
Coating	2	0.256768	0.128384	25.91	0.005
Error	4	0.019823	0.004956		
Total	8	0.372709			

Blade Run-in 15

MTB > ANOVA 'Force_15' = 'GroupNo' 'Coating'.

Analysis of Variance (Balanced Designs)

Factor	Type	Levels	Values
GroupNo	fixed	3	1 2 3
Coating	fixed	3	0 40 55

Analysis of Variance for Force_15

Source	DF	SS	MS	F	P
GroupNo	2	0.22113	0.11057	13.17	0.017
Coating	2	0.24238	0.12119	14.44	0.015
Error	4	0.03358	0.00839		
Total	8	0.49709			

Blade Run-in 20

MTB > ANOVA 'Force_20' = 'GroupNo' 'Coating'.

Analysis of Variance (Balanced Designs)

Factor	Type	Levels	Values
GroupNo	fixed	3	1 2 3
Coating	fixed	3	0 40 55

Analysis of Variance for Force_20

Source	DF	SS	MS	F	P
GroupNo	2	0.43835	0.21917	6.03	0.062
Coating	2	0.07822	0.03911	1.08	0.423
Error	4	0.14529	0.03632		
Total	8	0.66186			

Appendix E

Analysis of Viscosity

Blade Run-in 5

MTB > ANOVA 'Visco_5' = 'GroupNo' 'Coating'.

Analysis of Variance (Balanced Designs)

Factor	Type	Levels	Values
GroupNo	fixed	3	1 2 3
Coating	fixed	3	0 40 55

Analysis of Variance for Visco_5

Source	DF	SS	MS	F	P
GroupNo	2	27.72	13.86	0.73	0.537
Coating	2	1015.18	507.59	26.70	0.005
Error	4	76.03	19.01		
Total	8	1118.93			

Blade Run-in 10

MTB > ANOVA 'Visco_10' = 'GroupNo' 'Coating'.

Analysis of Variance (Balanced Designs)

Factor	Type	Levels	Values
GroupNo	fixed	3	1 2 3
Coating	fixed	3	0 40 55

Analysis of Variance for Visco_10

Source	DF	SS	MS	F	P
GroupNo	2	6.04	3.02	0.30	0.759
Coating	2	299.20	149.60	14.64	0.014
Error	4	40.88	10.22		
Total	8	346.13			

Blade Run-in 15

MTB > ANOVA 'Visco_15' = 'GroupNo' 'Coating'.

Analysis of Variance (Balanced Designs)

Factor	Type	Levels	Values
GroupNo	fixed	3	1 2 3
Coating	fixed	3	0 40 55

Analysis of Variance for Visco_15

Source	DF	SS	MS	F	P
GroupNo	2	2.069	1.034	0.11	0.900
Coating	2	112.809	56.404	5.92	0.064
Error	4	38.138	9.534		
Total	8	153.016			

Blade Run-in 20

MTB > ANOVA 'Visco_20' = 'GroupNo' 'Coating'.

Analysis of Variance (Balanced Designs)

Factor	Type	Levels	Values
GroupNo	fixed	3	1 2 3
Coating	fixed	3	0 40 55

Analysis of Variance for Visco_20

Source	DF	SS	MS	F	P
GroupNo	2	10.002	5.001	2.40	0.206
Coating	2	4.509	2.254	1.08	0.421
Error	4	8.324	2.081		
Total	8	22.836			

Appendix F

Calculation of Coat Weight

Table 1. For Water Loss Due to Evaporation

Coating →	40-A	40-B	40-C	0-A	0-B	0-C
Time(sec)	Weight of Film and Coating Color (in grams - WT)					
0	1.1741	1.2201	1.5518	1.7622	1.8646	1.5572
100	1.1616	1.2074	1.535	1.7518	1.8566	1.5496
200	1.1532	1.1986	1.5238	1.7454	1.8515	1.5444
300	1.1465	1.1921	1.5158	1.7409	1.8477	1.5407
400	1.1412	1.1872	1.5095	1.7375	1.8445	1.5378
500	1.1372	1.1834	1.5051	1.7346	1.8419	1.5354
600	1.1336	1.1803	1.5014	1.7323	1.8398	1.5334
Dry Film wt(WF)	0.9408	0.9718	1.2313	1.3906	1.5358	1.244

Coating →	40-A	40-B	40-C	0-A	0-B	0-C
Time(in sec)	Weight of Coating Color (in grams WT - WF)					
0	0.2333	0.2483	0.3205	0.3716	0.3288	0.3132
100	0.2208	0.2356	0.3037	0.3612	0.3208	0.3056
200	0.2124	0.2268	0.2925	0.3548	0.3157	0.3004
300	0.2057	0.2203	0.2845	0.3503	0.3119	0.2967
400	0.2004	0.2154	0.2782	0.3469	0.3087	0.2938
500	0.1964	0.2116	0.2738	0.344	0.3061	0.2914
600	0.1928	0.2085	0.2701	0.3417	0.304	0.2894
Time(in sec)	Water Loss of Coating Color (in %)					
0	0	0	0	0	0	0
100	5.4	5.1	5.2	2.8	2.4	2.4
200	9.0	8.7	8.7	4.5	4.0	4.1
300	11.8	11.3	11.2	5.7	5.1	5.3
400	14.1	13.3	13.2	6.6	6.1	6.2
500	15.8	14.8	14.6	7.4	6.9	7.0
600	17.4	16.0	15.7	8.0	7.5	7.6

Table 2.

Coat Weight After 400 sec (CW40).

Blade Run→	% Water loss (WL)	5			10			15			20		
		A	B	C	A	B	C	A	B	C	A	B	C
Coating 00	6.3		127	304			81	43	42	48	15	22	22
Coating 40	13.5	157	106	224	41	58	62	19	24	29	9.5		11
Coating 55	45.0	101	151	83	24	30	21	9.9	13	8.3	5.5	6.6	5.5

Wet Coat Weight (CW40*100/(100-WL))

Blade Run→	% Water loss (WL)	5			10			15			20		
		A	B	C	A	B	C	A	B	C	A	B	C
Coating 00	6.3		136	324			86	46	45	51	16	23	24
Coating 40	13.5	181	123	259	47	67	72	22	28	34	11		13
Coating 55	45.0	183	274	151	44	55	39	18	23	15	10	12	10

REFERENCES

1. Attal, J.F., and Roper III, J. A., "Evaluation of High-Speed Runnability using Pilot Coater Data, Rheological Measurements and Computer Modeling," Proceedings of 1993 TAPPI Coating Conference, TAPPI PRESS, Atlanta, GA, 1993, pp 107.

2. Eklund, D.E., and Kahila, S.J., "Factors influencing the Coat Weight in Blade Coating with Bevelled Blades Theory and Practice," Proceedings of 1978 TAPPI Coating Conference, TAPPI PRESS, Atlanta, GA, 1978, pp 13.

3. Bousfield, D.W., "Prediction of Velocity and Coat Weight limits based on Filter-cake formation," *Tappi Journal*, 77(7):161(1994) .

4. Follette, W.J., and Fowells, R.W., "Operating Variables of a Blade Coater," *Tappi Journal,* 43(11):953(1960).

5. Isaksson, P., Engstrom, G., and Rigdahl, M., "Experimental Analysis of the Dynamic Equilibirium in the vicinity of the Blade tip during Blade Coating,",*Nordic Pulp & Paper Research Journal,* 3(9):150(1994).

6. Engstrom, G., "Analysis of the Processes of Forming and Consolidation in Blade Coating," Proceedings of 1995 TAPPI Coating Fundamentals Symposium, TAPPI PRESS, Atlanta, GA, 1995, pp 41.

7. Chen, K.S.A., and Scriven, L.E., "On the Physics of Liquid Penetration into a Deformable Porous Substrate," Proceedings of 1993 TAPPI Coating Conference, TAPPI PRESS, Atlanta, GA, 1993, pp 93.

8. Beazley, K.M., and Windle W., "The Mechanics of Blade Coating," *Tappi Journal,* 50(1):1(1967).

9. Kuzmak, J.M., "Bevelled-Blade Coating," *Tappi Journal,* 43(2):72(1985).

10. McGenity P.M., Gane P.A.C., Watters P., "Factors Influencing the Runnability of Coating Colors at High Speed," Proceedings of 1992 TAPPI Coating Conference, TAPPI PRESS, Atlanta, GA, 1992, pp 117.

11. McGenity, P.M., Gane, P.A.C., Husband, J.C., and Engley, M.S., "Effect of Interactions between Coating Color Components on Rheology, Water Retention and Runnability," Proceedings of 1992 TAPPI Coating Conference, TAPPI PRESS, Atlanta, GA, 1992, pp 113.

12. Young, T.S., Pivonka, D.E., Weyer L.G., and Ching, B., "A Study of Coating Water Loss and Immobilization under dynamic conditions," Proceedings of 1993 TAPPI Coating Conference, TAPPI PRESS, Atlanta, GA, 1993, pp 223.

13. Eklund, D., and Letzelter, P., "Coating Color Dewatering in Blade coaters," Proceedings of 1993 TAPPI Coating Conference, TAPPI PRESS, Atlanta, GA, 1993, pp 247.

14. Gron, J.P.L., and Kline, J.E., "Rheological Properties of the Coating Colors influencing Variations in Surface Properties of the Coated Paper," Proceedings of 1993 TAPPI Coating Conference, TAPPI PRESS, Atlanta, GA, 1993, pp 235.

15. Chonde, Y., and Roper, J., "A review of Wet Coating Structure: Pigment/ Latex/ Cobinder interaction and its impact on Rheology and Runnability," Proceedings of 1995 TAPPI Coating Conference, TAPPI PRESS, Atlanta, GA, 1995, pp 57.

16. Barnes, H.A., Hutton, J.F., and Walters K., *An Introduction to Rheology*, second edition, Elsevier Science Publication Co., New York, 1989, pp11.

17. Krieger I.M., Buscall, Carver, Stegemen, *Polymer Colloids*, first edition, Elsevier Science Publication Co., New York, pp219.

18. Beazley, K.M., and Windle, W., "The Role of Viscoelasticity in Blade Coating," *Tappi Journal*, 51(8):340(1968) .

19. Triantafillopoulos, N., and Grankvist, T., "Viscoelasticity and High-Shear Viscosity of Coatings in relationship to Short Dwell Runnability," Proceedings of 1992 TAPPI Coating Conference, TAPPI PRESS, Atlanta, GA, 1992, pp 23.

20. Bliesner, W.C., "Basic Mechanism in Blade Coating," *Tappi Journal*, 54(10):1673(1971) .

21. Triantafillopoulos, N., and Atlug, N., "Experimental Evaluation Of the Forces in Bevelled Blade Coating," Proceedings of 1994 TAPPI Coating Conference, TAPPI PRESS, Atlanta, GA, 1994, pp 77.

22. Guler, E., and Bousfield, W. D., "Blade Force Measurements on a Laboratory Puddle Coater." M. S. thesis. University of Maine, 1994.

23. Cross M. M., "Flow Equation For Pseudoplastic Systems," *Colloid Science Journal*, 20:417(1965).

24. Gillespie T. J., "Viscosity Of Suspensions With Shear Thickening," *Colloid Science Journal*, 22: 554(1966).

25. Montgomery D.C., *Design and Analysis of Experiments*, Third Edition, Wiley, New York, 1994, pp14.